

Evolution of facial innervation in anomodont therapsids (Synapsida): Insights from X-ray computerized microtomography

Julien Benoit¹  | Kenneth D. Angielczyk^{1,2} | Juri A. Miyamae³ | Paul Manger⁴  | Vincent Fernandez⁵ | Bruce Rubidge¹

¹Evolutionary Studies Institute (ESI), School of Geosciences, University of the Witwatersrand, Johannesburg 2050, South Africa

²Integrative Research Center, Field Museum of Natural History, 1400 South Lake Shore Drive, Chicago, Illinois 60605

³Department of Geology & Geophysics, P.O. Box 208109, Yale University, New Haven, Connecticut 06520-8109

⁴School of Anatomical Sciences, University of the Witwatersrand, Johannesburg 2193, South Africa

⁵European Synchrotron Radiation Facility, Beamline ID19, Grenoble 38000, France

Correspondence

Julien Benoit, Evolutionary Studies Institute (ESI), School of Geosciences, University of the Witwatersrand, PO Wits, Johannesburg 2050, South Africa.

Email: julien.benoit@wits.ac.za

Abstract

Anomodontia was the most successful herbivorous clade of the mammalian stem lineage (non-mammalian synapsids) during the late Permian and Early Triassic. Among anomodonts, Dicynodontia stands apart because of the presence of an osseous beak that shows evidence of the insertion of a cornified sheath, the rhamphotheca. In this study, fourteen anomodont specimens were microCT-scanned and their trigeminal canals reconstructed digitally to understand the origin and evolution of trigeminal nerve innervation of the rhamphotheca. We show that the pattern of innervation of the anomodont “beak” is more similar to that in chelonians (the nasopalatine branch is enlarged and innervates the premaxillary part of the rhamphotheca) than in birds (where the nasopalatine and maxillary branches play minor roles). The nasopalatine branch is noticeably enlarged in the beak-less basal anomodont *Patranomodon*, suggesting that this could be an anomodont or chameleon synapomorphy. Our analyses suggest that the presence or absence of tusks and postcanine teeth are often accompanied by corresponding variations of the rami innervating the caniniform process and the alveolar region, respectively. The degree of ossification of the canal for the nasal ramus of the ophthalmic branch also appears to correlate with the presence of a nasal boss. The nasopalatine canal is absent from the premaxilla in the Bidentalida as they uniquely show a large plexus formed by the internal nasal branch of the maxillary canal instead. The elongated shape of this plexus in *Lystrosaurus* supports the hypothesis that the rostrum evolved as an elongation of the subnarial region of the snout. Finally, the atrophied and variable aspect of the trigeminal canals in *Myosaurus* supports the hypothesis that this genus had a reduced upper rhamphotheca.

KEY WORDS

anomodontia, beak, dicynodontia, maxillary canal, rhamphotheca

1 | INTRODUCTION

Anomodontia is a group of successful, mostly herbivorous therapsids, which first appear in the fossil record in the Wordian (middle Permian), about 265–270 million years ago (Ma) (Liu, Rubidge, & Li, 2010). The main subclade of anomodonts, Dicynodontia, rapidly radiated and became the most diverse and abundant tetrapod herbivores of the Lopingian (late Permian) and much of the Triassic (King, 1988; Ruta, Angielczyk, Fröbisch, & Benton, 2013). Anomodonts evolved a range of body sizes (from approximately mouse-sized to rhinoceros-sized) and ecomorphologies, including the arboreal *Suminia* (Fröbisch & Reisz, 2009, 2011), the fossorial cistecephalids (Cox, 1972; Cluver, 1978;

Nasterlack, Canoville, & Chinsamy, 2012; Laaß, 2015; Laaß & Schillinger, 2015; Laaß & Kaestner, 2017), and the possibly semi-aquatic *Lystrosaurus* (e.g., Ray, Chinsamy, & Bandyopadhyay, 2005; although see King, 1990). Some members of the clade may have evolved a parasagittal hindlimb posture, although the forelimbs appear to have retained a more sprawling posture (e.g., King, 1985; Fröbisch, 2006).

Although they suffered a significant loss in species richness (King, 1990; Fröbisch, 2008, 2013; Irmis & Whiteside, 2012), anomodonts survived the Permo-Triassic mass extinction and underwent a secondary diversification before finally going extinct near the end of the Triassic (Ruta et al., 2013). This gives the Anomodontia a temporal range of about 60 million years (and possibly over 100 million years if

controversial fossils from the Early Cretaceous of Australia truly represent a late-surviving dicynodont; Thulborn & Turner, 2003), the longest of any major non-mammalian synapsid clade. Finally, anomodonts were cosmopolitan, with their remains having been discovered on every continent (Fröbisch, 2009).

The most diverse and abundant subclade of Anomodontia is Dicynodontia. There are more than 100 well-characterized dicynodont species (Fröbisch, 2009) and in some areas, such as the upper Permian strata of the South African Karoo Basin, dicynodonts comprise 77%–96% of the specimens discovered (Sidor & Smith, 2007; Smith, Rubidge, & van der Walt, 2012). The dicynodont skull is highly modified, compared to the basic therapsid ground plan, to accommodate a palinal motion of the mandible associated with the adoption of a herbivorous diet (Watson, 1948; Crompton & Hotton, 1967; King, Oelofsen, & Rubidge, 1989). These modifications include a significantly shortened snout, a partial bony secondary palate formed primarily by the fused premaxillae, loss of premaxillary teeth and reduction or complete loss of the postcanine dentition, extreme reduction of the transverse flanges of the pterygoids, extensive emargination of the temporal openings, presence of a large lateral fossa on the squamosal hypothesized to accommodate a neomorphic jaw adductor muscle mass (*M. adductor mandibulae externus lateralis*; see Crompton & Hotton, 1967; Barghusen, 1986; King et al., 1989; King, 1994, Angielczyk, 2004), enlargement of the temporal opening, a jaw joint that allows extensive translation of the articular relative to the quadrate, and fusion of the mandibular symphysis. Based on the reduction or complete loss of premaxillary teeth, the presence of oblique canals and rugose bone texturing covering the premaxilla and the more rostral parts of the maxilla, and the presence of dense Sharpey's fibers in the premaxilla and maxilla, it is posited that a cornified beak, or ramphotheca, was present in dicynodonts (King, 1988, 1990; Hieronymus, Witmer, Tanke, & Currie, 2009; Jasinoski & Chinsamy-Turan, 2012).

A ramphotheca and the underlying edentulous bony beak is a striking evolutionary innovation which evolved multiple times in tetrapods (Lee, 1997). The presence of a ramphotheca has been inferred in Dicynodontia since the first description of members of the group (Owen, 1845), with taxonomic names such as *Dicynodon testudiceps* (now regarded as a *nomen dubium*; see Kammerer, Angielczyk, & Fröbisch, 2011), *Emydops*, and *Therochelonia* referring to the superficial similarity that exists between the beaks of dicynodonts and turtles.

In turtles and birds the osseous edentulous beak is covered by a cornified ramphotheca made of keratin. The ramphothecal tissue is a living structure supplied and innervated by numerous vessels and nerves that ramify inside the osseous beak, opening on its surface and giving a rugose texture to the external surface of maxilla, premaxilla, and palate (Witmer, 1995; Buchtová, Páč, Knotek, & Tichý, 2009; Hieronymus et al., 2009). Innervation by the somatosensory fibers of the trigeminal nerve (cranial nerve V, hereafter CNV), confers tactile sensitivity to the beak. The trigeminal nerve is divided into three main branches: the mandibular branch (CNV₃) innervates the mandible, whereas the maxillary (CNV₂) and ophthalmic (CNV₁) branches innervate the upper jaw (Owen, 1866; Dubbeldam, 1998; Witmer, 1995; Nieuwenhuys, Ten Donkelaar, & Nicholson, 1998; Higashiyama &

Kuratani, 2014). In turtles, the beak of the upper jaw is constituted by the maxilla laterally and the premaxilla medially and the ramphotheca is innervated by the nasopalatine ramus of CNV₂ (Figure 1; Owen, 1866). The beak of birds, in contrast, is formed primarily by the extended premaxilla, which is innervated by CNV₁, as in other archosaurs (Dubbeldam, 1998; Witmer, 1995). Each of these conditions differs in its own way from the plesiomorphic condition encountered in most amniotes, in which the snout is innervated by both CNV₁ and CNV₂, and the tooth roots are supplied and innervated by the maxillary canal, which transmits CNV₂ and accompanying vessels (Bellairs, 1949; Düring von & Miller, 1979; Witmer, 1995; Abdel-Kader, Ali, & Ibrahim, 2011; Leitch & Catania, 2012; Benoit, Manger, & Rubidge, 2016a).

Reconstructing the pathway of the trigeminal nerve fibers in extinct beaked taxa such as anomodonts will elucidate the adaptation of their nervous systems to the evolutionary innovation of a synapsid ramphotheca, as well as how facial sensitivity co-varies with the gradual reduction and disappearance of teeth. The aim of this study is thus to describe the patterns of ramification of the trigeminal canals in the upper jaw (CNV₁ and CNV₂) of anomodonts in order to address how innervation patterns in the snout co-evolved with the development of a cornified beak.

2 | MATERIAL AND METHODS

2.1 | Material scanned

2.1.1 | Anomodontia

- NMQR 3000: *Patranomodon nyaphulii* (Anomodontia), *Eodicynodon* Assemblage Zone (AZ), Karoo Basin, Wordian (middle Permian). Scanned at the ESI (Evolutionary Studies Institute) using Nikon Metrology XTH 225/320 LC. Voxel size: 0.036 mm,

- NMQR 2978: *Eodicynodon oosthuizeri* (Dicynodontia), *Eodicynodon* AZ, Karoo Basin, Wordian (middle Permian). Scanned at the ESI using Nikon Metrology XTH 225/320 LC. Voxel size: 0.074 mm,

- BP/1/2642: *Pristerodon mackayi* (Dicynodontia: Eumantelliidae), *Cistecephalus* AZ, Karoo Basin, Wuchiapigian (late Permian). Scanned at the ESI using Nikon Metrology XTH 225/320 LC. Voxel size: 0.0469 mm.

- NHCC LB314: *Abajudon kaayai* (Dicynodontia: Endothiodontia), lower Madumabisa Mudstone Formation, Mid-Zambezi Basin,? Capitanian (middle Permian). Scanned at the University of Chicago PaleoCT facility using GE v|tome|x s 240. Voxel size: 0.080 mm.

- SAM-PK-K11193: *Diictodon feliceps* (Dicynodontia: Pylaecephalidae), *Cistecephalus* AZ, Karoo Basin, Wuchiapigian (late Permian). Scanned at the ID19 beamline of the European Synchrotron Radiation Facility (ESRF, Grenoble). Voxel size: 0.0469 mm.

- NHCC LB14: *Compsodon helmoedi* (Dicynodontia: Emydopoidea), upper Madumabisa Mudstone Formation, Luangwa Basin, Wuchiapigian (late Permian). Scanned at the University of Chicago PaleoCT facility using GE v|tome|x s 240. Voxel size: 0.065 mm.

- BP/1/2690: *Myosaurus gracilis* (Dicynodontia: Emydopoidea), *Lystrosaurus* AZ, Karoo Basin, Induan (Early Triassic). Scanned at the ESI using Nikon Metrology XTH 225/320 LC. Voxel size: 0.0221 mm.

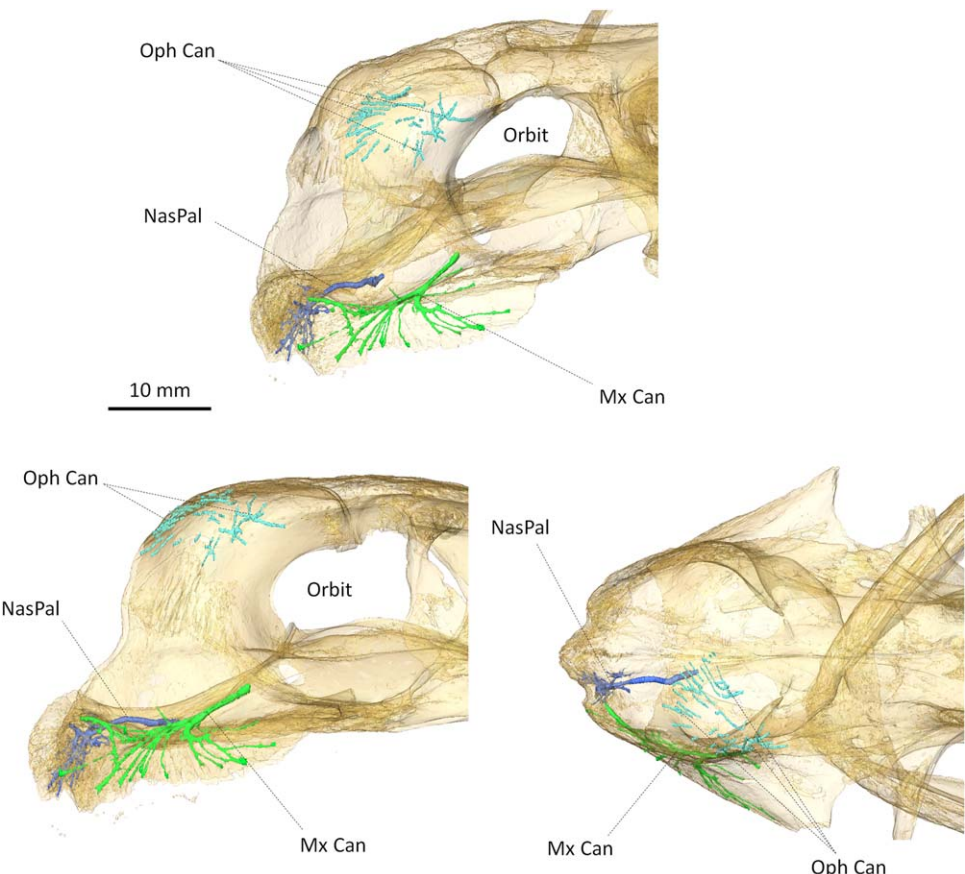


FIGURE 1 The trigeminal canals in the tortoise *Stigmochelys pardalis*. (BP/4/TAB). Top, oblique view; Left, lateral view; Right, dorsal view. The ophthalmic canal is light blue, the nasopalatine canal is dark blue and the maxillary canal is green. Abbreviations: Mx Can, maxillary canal; NasPal, nasopalatine canal; Oph Can, ophthalmic canal. Scale bar: 10 mm

- BP/1/2701a: *Myosaurus gracilis* (Dicynodontia: Emydopoidea), *Lystrosaurus* AZ, Karoo Basin, Induan (Early Triassic). Scanned at the ESI using Nikon Metrology XTH 225/320 LC. Voxel size: 0.0327 mm.
- BP/1/2701b: *Myosaurus gracilis* (Dicynodontia: Emydopoidea), *Lystrosaurus* AZ, Karoo Basin, Induan (Early Triassic). Scanned at the ESI using Nikon Metrology XTH 225/320 LC. Voxel size: 0.0234 mm.
- BP/1/4262: *Myosaurus gracilis* (Dicynodontia: Emydopoidea), *Lystrosaurus* AZ, Karoo Basin, Induan (Early Triassic). Scanned at the ESI using Nikon Metrology XTH 225/320 LC. Voxel size: 0.0221 mm.
- NHCC LB366: Cistecephalidae gen. et sp. nov. (Dicynodontia: Emydopoidea: Cistecephalidae), lower Madumabisa Mudstone Formation, Mid-Zambezi Basin, Capitanian or Wuchiapingian (middle or late Permian). Scanned at the University of Chicago PaleoCT facility using GE v|tome|x s 240. Voxel size: 0.041 mm.
- NHCC LB631: *Oudenodon bainii* (Dicynodontia: Cryptodontia: Oudenodontidae), upper Madumabisa Mudstone Formation, Luangwa Basin, Wuchiapingian (late Permian). Scanned at the University of Chicago PaleoCT facility using GE v|tome|x s 240. Voxel size: 0.010 mm.
- NMQR 3995: *Lystrosaurus curvatus* (Dicynodontia: Dicynodontoida: Lystrosauridae), *Lystrosaurus* AZ, Karoo Basin, Induan (Early Triassic). Scanned at the ESI using Nikon Metrology XTH 225/320 LC. Voxel size: 0.125 mm.

- NMQR 815: *Lystrosaurus declivis* (Dicynodontia: Dicynodontoida: Lystrosauridae), *Lystrosaurus* AZ, Karoo Basin, Induan (Early Triassic). Scanned at the ESI using Nikon Metrology XTH 225/320 LC. Voxel size: 0.086 mm.

2.1.2 | Outgroups

- CG-RMS353: *Heleosaurus scholtzi* (Eupelycosauria: Varanopidae); *Tapirocephalus* AZ, Karoo Basin, Capitanian (middle Permian). Scanned at the ESI using Nikon Metrology XTH 225/320 LC. Voxel size: 0.0378 mm.
- FMNH PR 1670: *Varanosaurus acutirostris* (Eupelycosauria: Ophiacodontidae); Wellington Formation, Oklahoma, Kungurian (early Permian). Scanned at the University of Chicago PaleoCT facility using GE v|tome|x s 240. Voxel size: 0.0663 mm.
- BP/1/3849: *Olivierosuchus parringtoni* (Therocephalia: Akidnognathidae); *Lystrosaurus* AZ, Karoo Basin, Induan (Early Triassic) Scanned at the ESI using Nikon Metrology XTH 225/320 LC. Voxel size: 0.0655 mm.
- BP/1/7199: *Thrinaxodon liorhinus* (Cynodontia: Epicynodontia); *Lystrosaurus* AZ, Karoo Basin, Induan (Early Triassic). Scanned at the ESRF (see Fernandez et al., 2013 for details). Voxel size: 0.03 mm.
- BP/4/1104: *Homopus* sp. (Chelonia: Testudinidae), extant, South Africa. Scanned at the ESI using Nikon Metrology XTH 225/320 LC. Voxel size: 0.0445 mm.

- BP/4/TAB no ref: *Stigmochelys pardalis* (Chelonia: Testudinidae), extant, South Africa. Scanned at the ESI using Nikon Metrology XTH 225/320 LC. Voxel size: 0.0513 mm.

- BP/4/1094: *Stigmochelys pardalis* (Chelonia: Testudinidae), extant, South Africa. Scanned at the ESI using Nikon Metrology XTH 225/320 LC. Voxel size: 0.0586 mm.

For enquiries concerning access to CT scan data, please contact K. Angielczyk or W. Simpson (wsimpson@fieldmuseum.org) for FMNH and NHCC specimens, and K. Jakata (kudawashe.jakata@wits.ac.za) for other specimens.

2.2 | Reconstruction of the trigeminal canals

Three-dimensional renderings of the internal structure of the maxillary and ophthalmic branches of the trigeminal nerve were obtained using manual segmentation in Avizo 8 (FEI VSG, Hillsboro, OR). Because we focus on the bony structures that transmitted tissues actively playing a role in the innervation and nutrition of the face, and thus are relevant to the evolution of beak sensitivity in anomodonts, we only segmented the parts of the canals that directly communicate with the external surface of the skull. In accordance with the phylogenetic relationship unifying Mammaliaformes and non-mammalian synapsids (NMS), and to maximize primary hypotheses of homology, our identifications of the rami of the trigeminal canals use the names of the corresponding rami of CNV in extant mammals. Note that some vessels and branches of the facial nerve (CNVII) may have shared the canal along with CNV and participated in the innervation and supply of the beak (Bellairs, 1949; Düring von & Miller, 1979; Witmer, 1995; Abdel-Kader et al., 2011; Leitch & Catania, 2012; see Benoit et al., 2016a). Mandibles were not preserved in some of the specimens examined here, and because the mandibular canal shows little variation, our descriptions focus on the upper jaw.

To investigate the evolution of the trigeminal canals and associated structures in dicynodonts, we used parsimony to optimize a series of 11 discrete-state characters (Supplementary Information 1) on a modified version of the phylogeny of Angielczyk and Kammerer (2017; the position of *Abajudon* is based on the results of Olroyd, Sidor, & Angielczyk, in press). We conducted the analysis using Mesquite version 3.2 (build 801) (Maddison & Maddison, 2017). Given the nature of our sampling, the non-bidentalian portion of the tree is the same as in Angielczyk and Kammerer (2017), but only two members of Bidentalia (*Oudenodon* and *Lystrosaurus*) are included.

This research complies with the legal requirements of the countries in which it was undertaken. No permits were required.

Institutional abbreviations: AMNH: American Museum of Natural History (New York City, U.S.A.); BP: Evolutionary Studies Institute (Johannesburg, South Africa); CG: Council for Geoscience (Pretoria, South Africa); FMNH: Field Museum of Natural History (Chicago, U.S.A.); NHCC: National Heritage Conservation Commission (Lusaka, Zambia); NMQR: National Museum (Bloemfontein, South Africa); SAM: Iziko Museum of Natural History South Africa (Cape Town, South Africa).

2.3 | Results

2.3.1 | Outgroups

Pelycosaur-grade synapsids are represented by the varanopid *Heleosaurus* (CG-RMS353; a complete left maxilla and fragments of the premaxilla, nasal, and frontals) and the ophiacodontid *Varanosaurus* (FMNH PR 1670; a complete, articulated skull and mandible). Non-anomodont therapsids are represented by the cynodont *Thrinaxodon* (BP/1/7199; complete and undistorted skull) and the therocephalian *Olivierosuchus* (BP/1/3849; Benoit et al., 2016a). Information on the trigeminal canals of additional non-anomodont therapsids can be found in Benoit et al. (2016a), but are not considered in detail here because *Olivierosuchus* and *Thrinaxodon* are generally representative of the morphologies found in those taxa.

In all four outgroup taxa, the surface of the bones forming the snout is smooth. The region normally innervated and supplied by the ophthalmic nerve and accompanying vessels is not preserved in *Heleosaurus*, but the ophthalmic canal was probably not ossified, as in most other NMS (Figure 2; Benoit et al., 2016a). The nasal ramus of the ophthalmic branch appears as a long, slender, and weakly ramified sulcus in *Varanosaurus*, but the frontal ramus is not completely enclosed in a bony tube (Figure 3). Instead, the frontal bone is pierced by minute foramina for the exit of the ophthalmic nerve (Figure 3; Benoit et al., 2016a). In place of an ophthalmic branch, *Olivierosuchus* displays isolated foramina only (Figure 4a). In contrast, a reasonably ossified path for both rami of the ophthalmic nerve is preserved in *Thrinaxodon*. The ophthalmic canal is divided into a caudal branch (the frontal rami) and a rostral branch (the nasal rami), which themselves ramify into numerous smaller canals that are oriented anteroposteriorly and open on the surface of the frontal and nasal bones, respectively (Figure 4b; Benoit et al., 2016a).

As in mammals (Rodella, Buffoli, Labanca, & Rezzani, 2012; Higashiyama & Kuratani, 2014), but unlike non-avian sauropsids (hereafter referred to as reptiles) and birds (Bellairs, 1949; Düring von & Miller, 1979; Witmer, 1995; Abdel-Kader et al., 2011; Leitch & Catania, 2012), the innervation and supply of the surface of the premaxilla is not provided by the ophthalmic canal in *Thrinaxodon* and *Olivierosuchus*. There are few neurovascular foramina on the premaxilla, which are so small that the corresponding canals are nearly invisible in the microCT data without high contrast and high resolution. As a result, they were overlooked in most previous microCT scan-based studies of the trigeminal innervation of the snout in therapsids (Crompton, Musinsky, & Owerkowicz, 2015; Crompton, Owerkowicz, Bhullar, & Musinsky, 2017; Benoit et al., 2016a, b; Laaß & Kaestner, 2017). In *Thrinaxodon* and *Olivierosuchus*, the premaxillary neurovascular foramina are connected to a short tube that originates from the premaxillary portion of the roof of the oral cavity, and which therefore may have been for the nasopalatine nerve (Figure 4). In *Thrinaxodon*, this tube is connected to the internal nasal ramus of the maxillary canal laterally, which suggests that the maxillary nerve might have contributed to the innervation of the premaxillary surface as well (Figure 4b). This condition is likely not representative of the plesiomorphic condition in synapsids as it is shared with Mammalia, in which the surface of the premaxilla is also

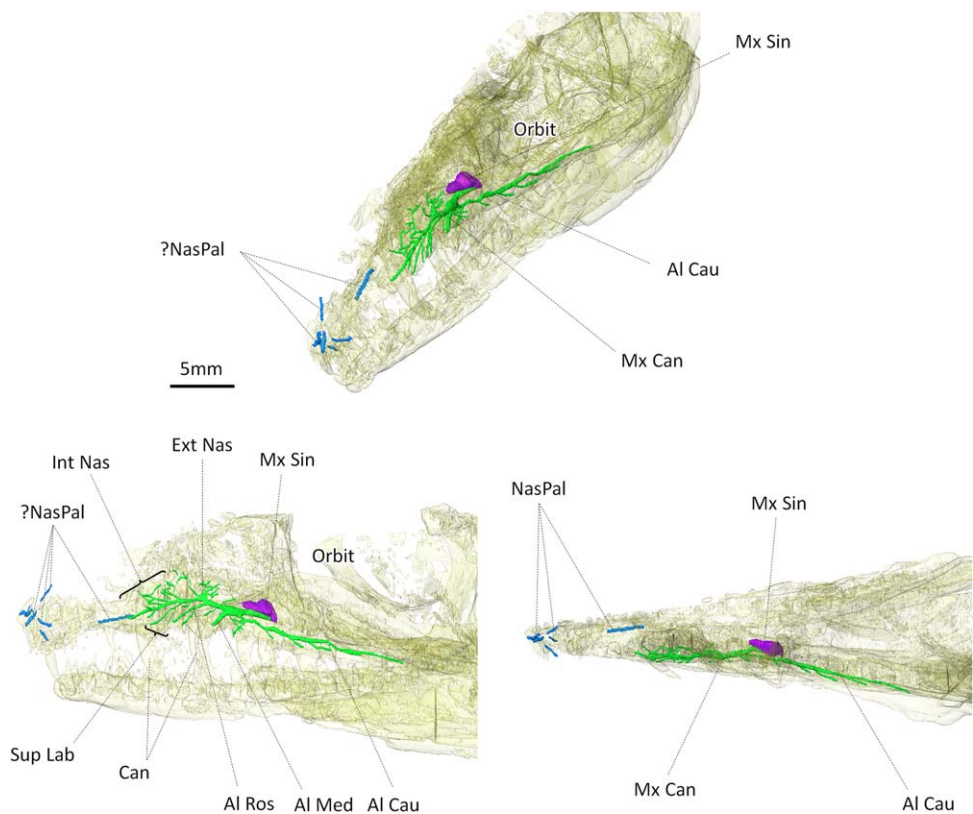


FIGURE 2 The trigeminal canals in *Heleosaurus scholtzi*. (CG-RMS353). Top, oblique view; Left, lateral view; Right, dorsal view. The nasopalatine canal is in dark blue and the maxillary canal is in green. Abbreviations: Al Cau, caudal alveolar ramus; Al Med, medial alveolar ramus; Al Ros, rostral alveolar ramus; Can, canine; Ext Nas, external nasal ramus; Int Nas, internal nasal ramus; Mx Can, maxillary canal; Mx Sin, maxillary sinus; NasPal, nasopalatine canal; Sup Lab, superior labial ramus. Scale bar: 5 mm

innervated by the maxillary nerve (Rodella et al., 2012; Higashiyama & Kuratani, 2014). In *Heleosaurus*, *Varanosaurus*, and *Olivierosuchus*, there is evidence of foramina on the premaxilla. In *Varanosaurus* and *Olivierosuchus*, where the premaxilla is better preserved, these foramina are connected to a network of thin canals which cluster caudally into a single opening on the buccal surface of the premaxilla (Figures 3, 4a). Therefore, these canals are here identified as the nasopalatine canal (Figures 3, 4a). However, unlike the more derived *Thrinaxodon* and mammals, the nasopalatine canal does not anastomose with the internal nasal ramus of the maxillary canal in *Varanosaurus* and *Olivierosuchus* (Figures 3, 4a), likely representing the plesiomorphic condition for synapsids.

Of the three branches of the trigeminal canals, the maxillary canal bears the largest number of identifiable rami. It is remarkable that its branches in the 'pelycosaurs,' *Heleosaurus*, and *Varanosaurus*, can be homologized with those of therapsids and mammals despite the fact that these taxa diverged from the lineage including mammals in the Pennsylvanian, over 300 million years ago. Rostrally, there are three major ramifications. The dorsal-most ramification is the external nasal ramus, which ramifies within the thickness of the maxilla at the level of the caniniform teeth (Figure 2). This branch innervates and supplies most of maxilla's surface in 'pelycosaurs' and other NMS (Figures 2–4; Benoit et al., 2016a). The rostral-most branch is the internal nasal ramus, which innervates and supplies the maxilla lateral to the naris.

This ramus sends a long branch medially that anastomoses with the nasopalatine canal in *Thrinaxodon* but not in other outgroup taxa (Figures 2–4a). Rostro-ventrally, there is the superior labial ramus, which innervates the rostro-ventral margin of the maxilla lateral to the naris (Figures 2–4).

Caudally, the maxillary canal is connected to the maxillary sinus (or maxillary antrum), a diverticulum of the nasal cavity (Figures 2–4). The maxillary sinus excavates a small space inside the internal wall of the maxilla, rostral to the orbit, in *Heleosaurus* and *Thrinaxodon* (Figures 2–4a), but it can be relatively extensive, as in *Varanosaurus*, *Olivierosuchus*, and some other NMS (Figures 3, 4b; Benoit et al., 2016a).

Between the maxillary sinus and the external nasal ramus, the maxillary canal ramifies into three distinct branches, the rostral, median, and caudal alveolar rami, in *Thrinaxodon*, *Olivierosuchus*, *Heleosaurus*, and the great majority of other NMS (Figures 2, 4; Benoit et al., 2016a). A median alveolar ramus was not identifiable in *Varanosaurus* (Figure 3), although it was likely present. The alveolar rami innervate the ventral margin of the maxilla above the postcanine teeth (Figures 2–4). In non-prostostodontian cynodonts, the caudal ramus (and in some cases, the median ramus) originates directly from the maxillary antrum, whereas in other, more stemward therapsids and the 'pelycosaurs,' all three rami originate from the maxillary canal (Figures 2–4; Benoit et al., 2016a). The most noticeable difference between the maxillary canal of 'pelycosaurs' and that in therapsids is the extension of

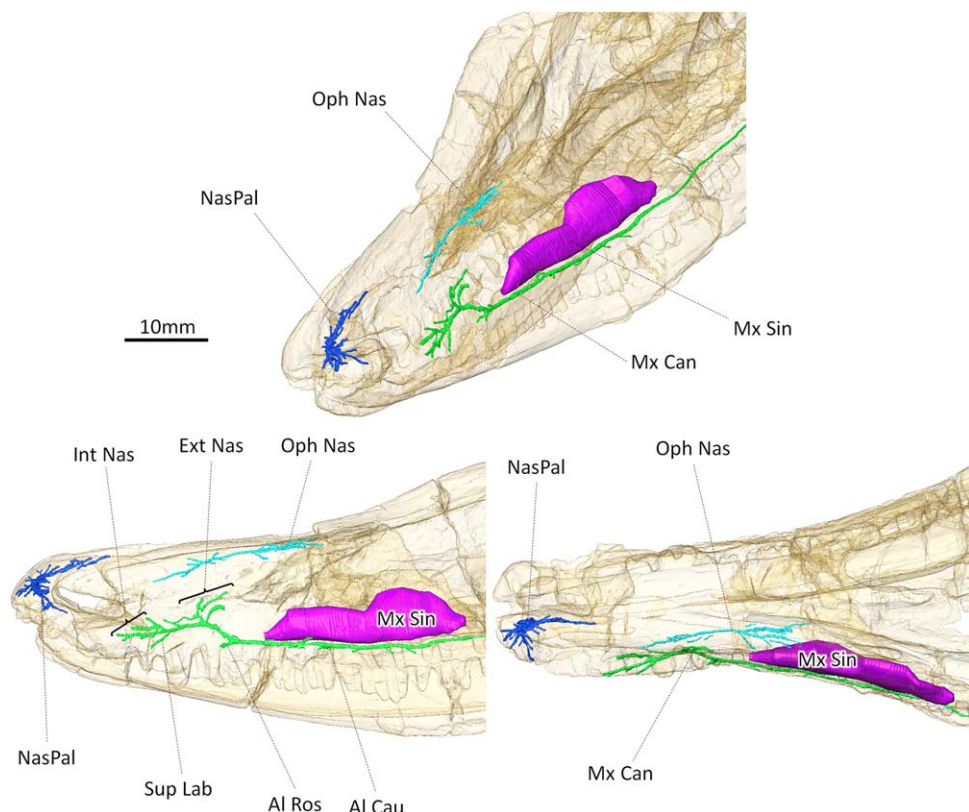


FIGURE 3 The trigeminal canals in *Varanosaurus acutirostris* (FMNH PR 1670). Top, oblique view; Left, lateral view; Right, dorsal view. The ophthalmic canal is in light blue, the nasopalatine canal is in dark blue and the maxillary canal is in green. Abbreviations: Al Cau, caudal alveolar ramus; Al Ros, rostral alveolar ramus; Ext Nas, external nasal ramus; Int Nas, internal nasal ramus; Mx Can, maxillary canal; Mx Sin, maxillary sinus; NasPal, nasopalatine canal; Oph Nas, nasal ramus of the ophthalmic canal; Sup Lab, superior labial ramus; Scale bar: 10 mm

the caudal alveolar ramus in ‘pelycosaurs.’ In *Heleosaurus* and *Varanosaurus*, the caudal alveolar ramus is lengthened caudally and gives off side branches at regular intervals that lead to the surface of the maxilla above the superior lip (Figures 2, 3). This results in the presence of regularly spaced foramina aligned parallel to the ventral margin of the maxilla that are strikingly reminiscent of the condition commonly encountered in reptiles (Owen, 1866; Bellairs, 1949; Estes, 1961; Tatarinov, 1976; Düring von & Miller, 1979; Brochu, 2003; Witmer, 1995; Abdel-Kader et al., 2011; Leitch & Catania, 2012; Benoit et al., 2016a; Barker, Naish, Newham, Katsamenis, & Dyke, 2017).

2.3.2 | Anomodontia

Patranomodon nyaphulii

Patranomodon is the basal-most anomodont in our sample (e.g., Kammerer et al., 2011; Castanhinha et al., 2013; Cox & Angielczyk, 2015; Angielczyk & Kammerer 2017), and is represented by a nearly complete and undeformed skull (NMQR 3000). Only the premaxillae are broken, and the acid used to prepare the skull might have infiltrated and enlarged the trigeminal canals. Therefore, some connections between the branches might not represent real anastomosis, but artifacts of acid preparation. As preserved, the bones on the snout are smooth, but the presence of rugosity on the rostral aspect of the premaxilla cannot be assessed.

Aside from two foramina on the dorsomedial surface of the nasal (Figure 5), the ophthalmic canal is not ossified in this species, as usual for NMS (Benoit et al., 2016a). The nasopalatine canal is not completely preserved because of the breakage of the premaxillae, but enough is visible to state that the nasopalatine nerve and accompanying vessels were transmitted by a sulcus on the dorsal surface of the buccal cavity and then ramified within the premaxilla to innervate the top of the snout (Figure 5). This condition greatly differs from that in the synapsid outgroup taxa, in which the nasopalatine canal leaves no sulcus inside the buccal cavity and thus appears shorter (Figures 2–4), but it is similar to the morphology encountered in chelonians (Figure 1).

The morphology of the maxillary canal of *Patranomodon* is similar to that in the outgroup taxa. There are three main ramifications: the internal nasal and superior labial rami, which pass through the maxilla and reach the anterior and ventral margins of the maxilla, respectively, and the external nasal ramus, which bears an extra ramification that extends far dorso-caudally toward the orbit (Figure 5). To date, such a lengthened extra ramification has been encountered only in the dinocephalian *Moschops* (Benoit, Manger, Norton, Fernandez, & Rubidge, 2017a). This observation is interesting given that dinocephalians and anomodonts often were considered to be closely related in the older literature (e.g., Broom, 1932; Watson, 1948; Watson & Romer, 1956; King, 1988), but further investigation of how widespread this

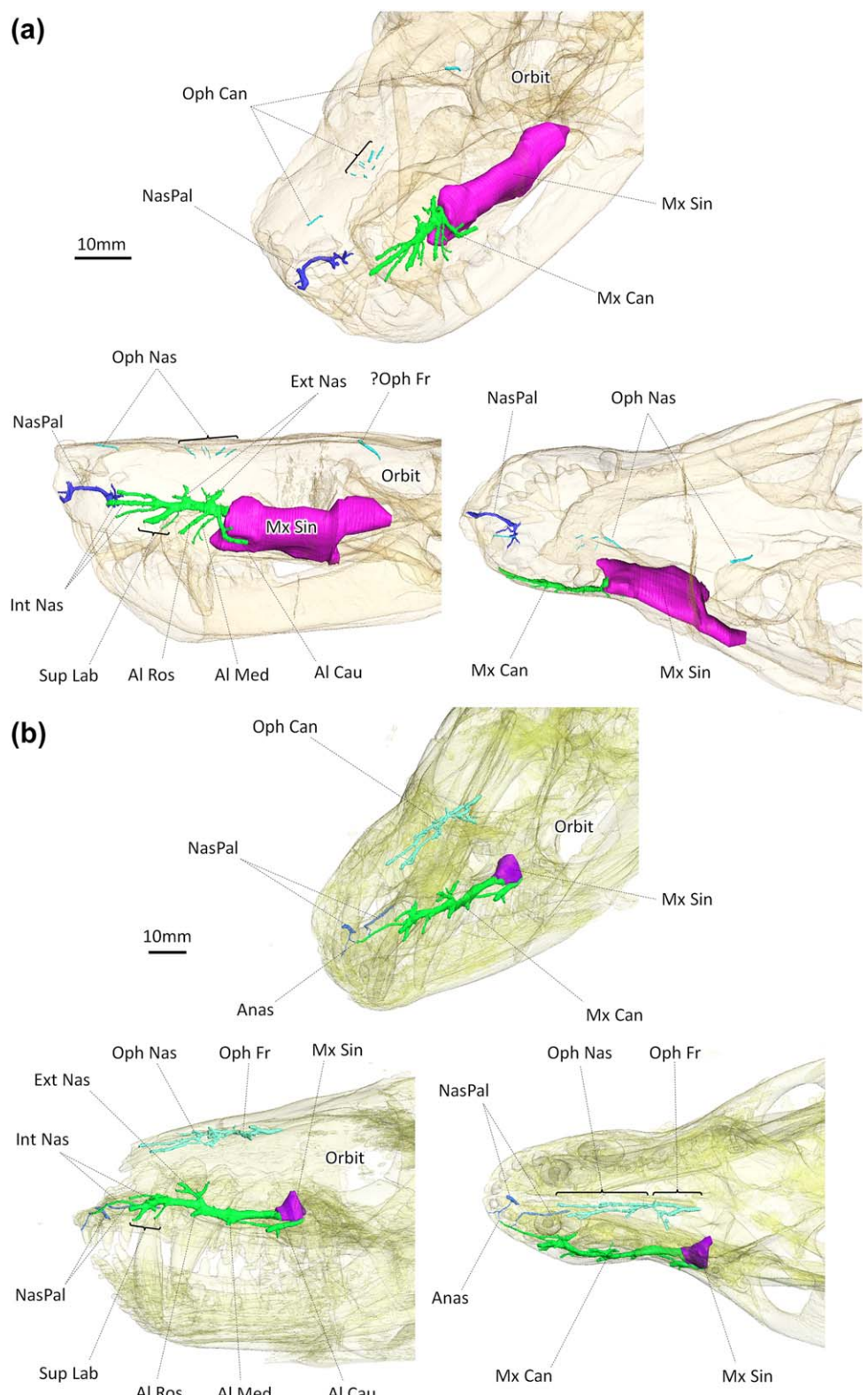


FIGURE 4 The trigeminal canals in *Oliverosuchus parringtoni* (A. BP/1/3849) and *Thrinaxodon liorhinus* (B. BP/1/7199). Top, oblique view; Left, lateral view; Right, dorsal view. The ophthalmic canal is in light blue, the nasopalatine canal is in dark blue and the maxillary canal is in green. Abbreviations: Al Cau, caudal alveolar ramus; Al Med, medial alveolar ramus; Al Ros, rostral alveolar ramus; Anas: anastomosis; Ext Nas, external nasal ramus; Int Nas, internal nasal ramus; Mx Can, maxillary canal; Mx Sin, maxillary sinus; NasPal, nasopalatine canal; Oph Can, ophthalmic canal; Oph Fr, frontal ramus of the ophthalmic canal; Oph Nas, nasal ramus of the ophthalmic canal; Sup Lab, superior labial ramus. Scale bars: 10 mm

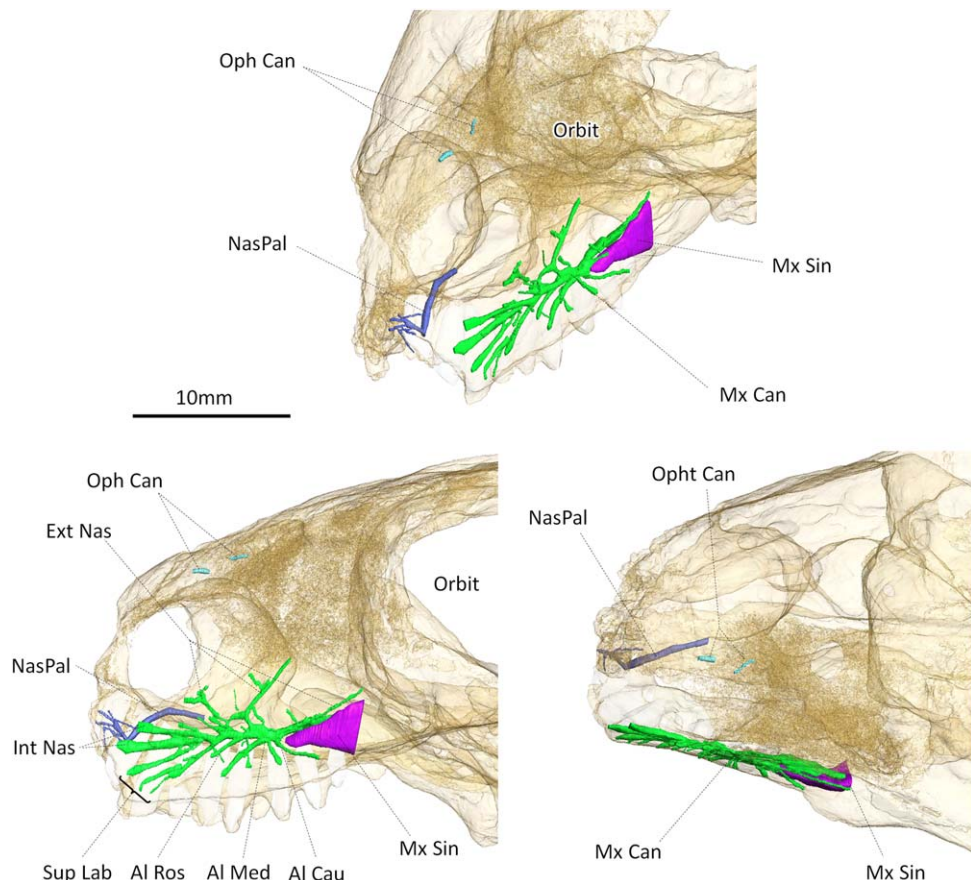


FIGURE 5 The trigeminal canals in *Patranomodon nyaphulii* (NMQR 3000). Top, oblique view; Left, lateral view; Right, dorsal view. The ophthalmic canal is in light blue, the nasopalatine canal is in dark blue and the maxillary canal is in green. Abbreviations: Al Cau, caudal alveolar ramus; Al Med, medial alveolar ramus; Al Ros, rostral alveolar ramus; Anas: anastomosis; Ext Nas, external nasal ramus; Int Nas, internal nasal ramus; Mx Can, maxillary canal; Mx Sin, maxillary sinus; NasPal, nasopalatine canal; Oph Can, ophthalmic canal; Sup Lab, superior labial ramus. Scale bar: 10 mm. Mirrored for comparison

mophology is in dinocephalians and non-dicynodont anomodonts will be needed before its phylogenetic significance can be fully assessed.

There are three alveolar rami that supply and innervate the facial surface above the complete set of cheek-teeth (Figure 5). As is usual in non-cynodont therapsids, the alveolar rami ramify from the maxillary canal and not from the maxillary sinus (Figure 5). Nevertheless, the condition in *Patranomodon* is slightly different from that in other therapsids because all three alveolar rami radiate from the same point within the maxillary canal (Figure 5). The maxillary sinus is incompletely ossified posteriorly, as in the outgroup taxa (Figure 5; Benoit et al., 2016a).

Eodicyndon oosthuizeni

Eodicyndon is the oldest and most stemward dicynodont in our sample (e.g., Rubidge, 1990a; Kammerer et al., 2011; Castanhinha et al., 2013; Cox & Angielczyk, 2015; Angielczyk, Hancox, & Nabavizadeh, in press; Angielczyk & Kammerer, 2017). It is represented by a complete, acid-prepared skull (NMQR 2978). As in all other dicynodonts (see descriptions below), the presence of a ramphotheca is evidenced by the rugose external surfaces of the premaxilla and maxilla (Rubidge, 1984, 1990b). The terminal openings of the numerous ramifications of the

trigeminal canal contribute to this rugosity, but it appears to be mostly caused by independent vascular canals that originate in the medullary cavities of the bones (Figure 6).

Only the nasal ramus of the ophthalmic nerve is ossified in *Eodicyndon* (Figure 6). It is moderately ramified, with canals oriented in all directions, and the longest branch rostrally reaches the posterior margin of the naris (Figure 6).

As in the basal anomodont *Patranomodon*, the nasopalatine nerve has numerous ramifications that connect to a long antero-posterior sulcus that excavates the roof of the oral cavity on the ventral surface of the palatal portion of the premaxilla. Along its course in the buccal cavity, the nasopalatine nerve may have given rise to branches that innervated the palate, but this is not evidenced on the specimen (Figure 6). Rostrally, the nasopalatine nerve penetrates the caudo-ventral margin of the premaxilla and ramifies into numerous smaller canals to innervate and supply the rostral extremity of the beak medial to the naris (Figure 6).

The maxillary canal is distinctive compared to that of the contemporaneous *Patranomodon*. Rostro-ventrally, the numerous branches of the superior labial ramus diverge inside the caniniform process rostral to the enlarged caniniform tusk (Figure 6). Rostrally, the internal nasal

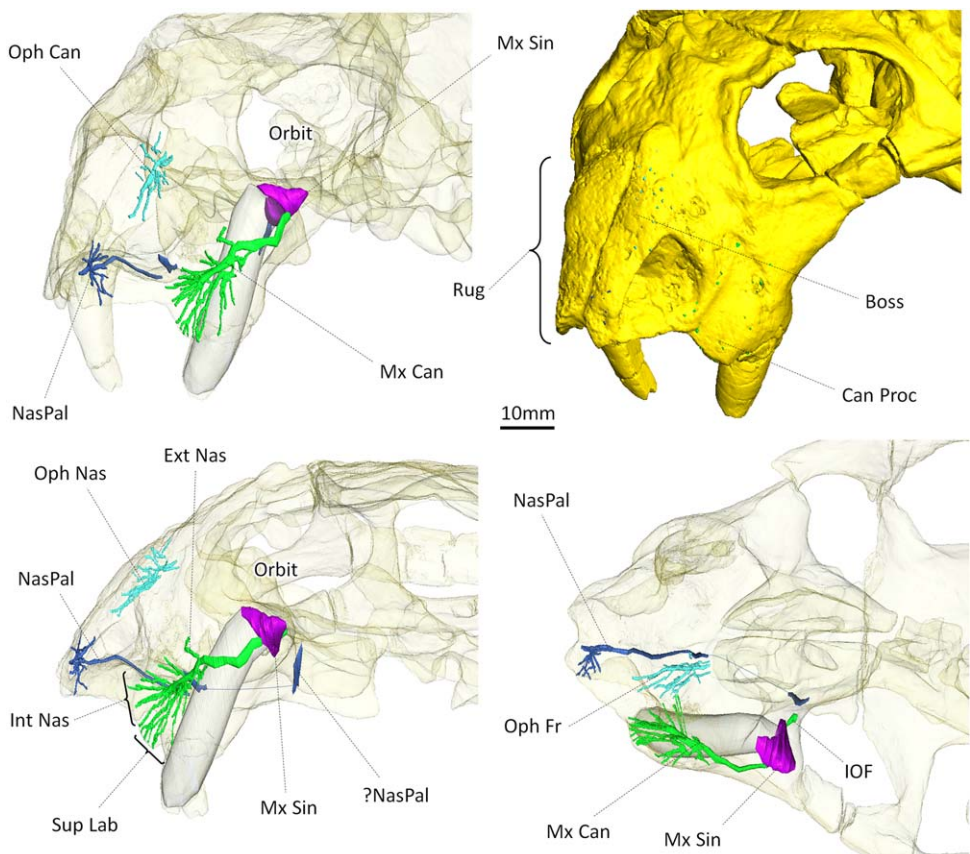


FIGURE 6 The trigeminal canals in *Eodicyodon oosthuizeni* (NMQR 2978). Top left, transparent skull in oblique view; Top right, solid skull in oblique view; Bottom left, lateral view; Bottom right, dorsal view. The ophthalmic canal is in light blue, the nasopalatine canal is in dark blue and the maxillary canal is in green. Abbreviations: Boss, nasal boss; Ext Nas, external nasal ramus; Int Nas, internal nasal ramus; IOF, infraorbital foramen; Mx Can, maxillary canal; Mx Sin, maxillary sinus; NasPal, nasopalatine canal; Oph Can, ophthalmic canal; Oph Fr, frontal ramus of the ophthalmic canal; Oph Nas, nasal ramus of the ophthalmic canal; Rug, rugosities of the ramphotheca; Sup Lab, superior labial ramus; Scale bar: 10 mm. Mirrored for comparison

ramus is highly ramified, and it innervates and supplies the maxillary part of the beak, lateral to the naris (Figure 6). In contrast, there is only one recognizable branch of the external nasal ramus, which ramifies dorsal to the tusk (Figure 6). The internal and external nasal rami are separated by a short, non-ramified portion of the maxillary canal (Figure 6).

Unlike in *Patranomodon* and other NMS, there are no alveolar rami in *Eodicyodon* (Figure 6), a condition that may be correlated to the near absence of postcanine teeth (only one postcanine tooth is present on the left side in NMQR 2978) (see Witmer, 1995; Benoit, Norton, Manger, & Rubidge, 2017b, for similar conditions in other taxa with reduced dentitions). However, the greatly enlarged caniniform tusk strongly affects the morphology of the maxillary sinus, which is mostly occupied by the tusk's root (Figure 7a). Caudal to the maxillary sinus, there is a discrete and ossified orbital opening for CNV₂, the infraorbital foramen, inside the orbit (Figure 7), a condition that is otherwise encountered only in probainognathian cynodonts (Benoit et al., 2016a).

Diictodon feliceps

Diictodon is a pylaecephalid dicynodont and is represented by a complete skull (SAM-PK-K11193). As in *Eodicyodon*, the terminal openings

of the trigeminal canals are located on the region of the snout that bears the rugosity associated with the ramphotheca (Figure 8).

The nasal ramus of the ophthalmic canal is partially ossified only at the level of the nasal boss (Figure 8). The rostral-most ramifications of the nasal ramus reach the posterior margin of the naris, as in *Eodicyodon* (Figure 8).

The nasopalatine canal richly innervates and supplies the extremity of the beak, medial to the naris (Figure 8). As in *Eodicyodon* there is a distinct sulcus for the nasopalatine nerve on the buccal surface of the palatal portion of the premaxilla.

The maxillary canal is less ramified distally but has a much more complex pattern of major branches compared to *Eodicyodon*. The internal nasal ramus is lengthened rostrally, elongated rostro-ventrally beyond the level of the naris, and anastomoses with the nasopalatine canal (Figure 8). Therefore, the maxillary canals likely participated to some degree in the irrigation and innervation of the surface of the premaxilla in *Diictodon*. This condition resembles that in the outgroup taxa and Bidentalalia (see below), although the internal nasal ramus of *Diictodon* does not seem to form the highly ramified plexus in the premaxilla that is present in *Lystrosaurus* and *Oudenodon*. As in *Eodicyodon*, the superior labial ramus ramifies rostrally inside the caniniform process

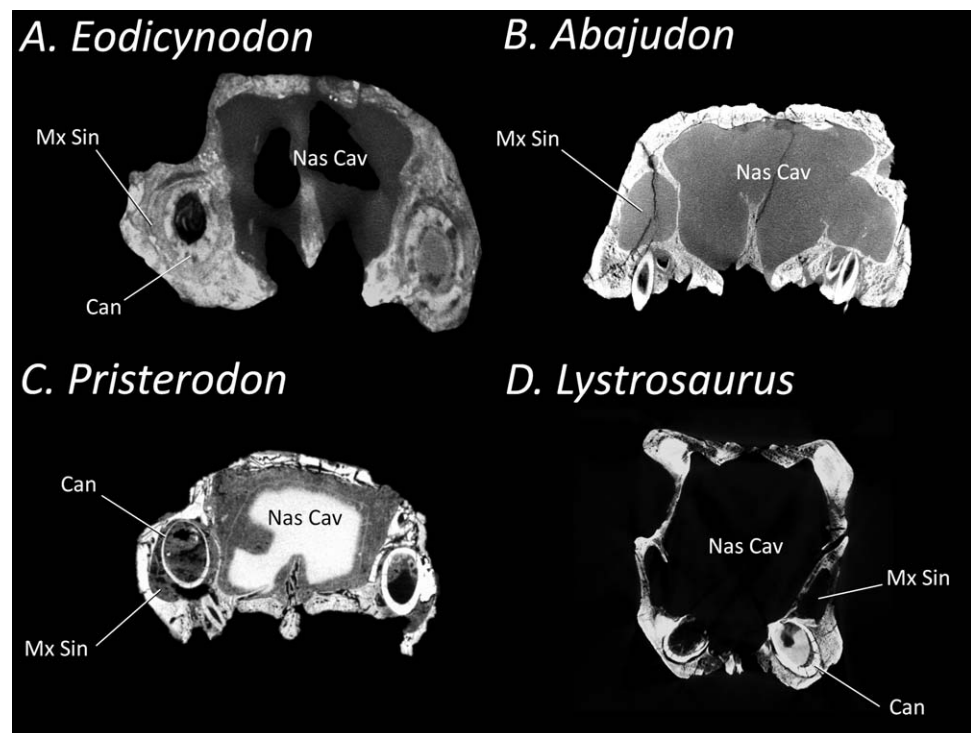


FIGURE 7 MicroCT slides to show the relationship of the maxillary canal and the canine root in coronal cross section. (a) *Eodicynodon* (NMQR 2978); (b) *Abajudon* (NHCC LB314); (c) *Pristerodon* (BP/1/2642); (d) *Lystrosaurus* (NMQR 815). Not to scale. Abbreviations: Can, canines; Mx Sin, maxillary sinus; Nas Cav, nasal cavity

(Figure 8). Caudally, the external nasal ramus ramifies at the level of the canine into four branches that are directed dorsally (Figure 8). Notably, the points where the external and internal nasal rami branch are separated by a long segment of the maxillary canal, a condition also encountered in *Pristerodon*, *Oudenodon*, and *Lystrosaurus*.

There are no postcanine teeth and no corresponding alveolar rami, as in *Lystrosaurus*, and the maxillary sinus is occupied by the large root of the tusk (Figure 8). There is no trace of an infraorbital foramen.

Pristerodon mackayi

Pristerodon is the sole member of the monotypic family Eumantelliidae (Kammerer & Angielczyk, 2009), and is a relatively basal dicynodont although its exact phylogenetic position has been difficult to reconstruct confidently (see discussion of this problem in Angielczyk, Rubidge, Day, & Lin, 2016). In this study, *Pristerodon* is represented by a complete acid-prepared skull (BP/1/2642), a specimen of historical importance because of the central role it played in Crompton and Hotton's (1967) analysis of the dicynodont feeding system. As in *Eodicynodon*, the terminal openings of the trigeminal canals contribute to the rugosity of the premaxilla and the anterior aspect of the maxilla (Figure 9).

Only a small part of the nasal ramus of the ophthalmic canal is ossified, but unlike in *Eodicynodon*, it does not reach the posterior border of the naris (Figure 9). The ramifications are mostly oriented antero-posteriorly (Figure 9).

There is a long and distinctive sulcus on the buccal surface of the palatal portion of the premaxilla for the nasopalatine nerve (Figure 9).

As in *Eodicynodon*, it penetrates the nasopalatine canal on the postero-ventral margin of the premaxilla (Figure 9). The dorsal branch arises from the nasopalatine canal immediately after it enters the premaxilla, after which the canal ramifies into numerous smaller canals more rostrally (Figure 9). These smaller branches extend to the external surface of the premaxilla, medial to the naris (Figure 9).

The maxillary canal innervates and supplies the maxilla lateral to the naris. Rostrally, the internal nasal ramus divides into three branches, one dorsally and two rostro-ventrally, which reach the lateral margin of the naris rostrally (Figure 9). The superior labial ramus ramifies rostro-ventrally inside the caniniform process, rostral to the tusk (Figure 9). Compared to *Eodicynodon*, the maxillary canal is lengthened between the point of ramification of the external nasal ramus and that of the internal nasal ramus (Figure 9). The external nasal ramus branches at the level of the canine, and it innervates and supplies the surface of the maxilla dorso-rostrally to the canine (Figure 9). Caudally, the maxillary canal passes through the maxillary antrum and opens inside the orbit through a discrete infraorbital foramen (Figure 9).

There are three distinct alveolar rami (Figure 9). The caudal ramus is short and originates directly from the ventral surface of the orbit (Figure 9). The medial ramus is connected to a deep sulcus that excavates the ventral margin of the maxillary sinus, which might represent the course of the maxillary nerve through this antrum (Figure 9). The medial ramus separates from this sulcus at the level of the only complete postcanine tooth preserved, and finishes its course on the surface of the maxilla just caudal to the canine (Figure 9). The rostral alveolar ramus branches just posterior to the canine and innervates the same

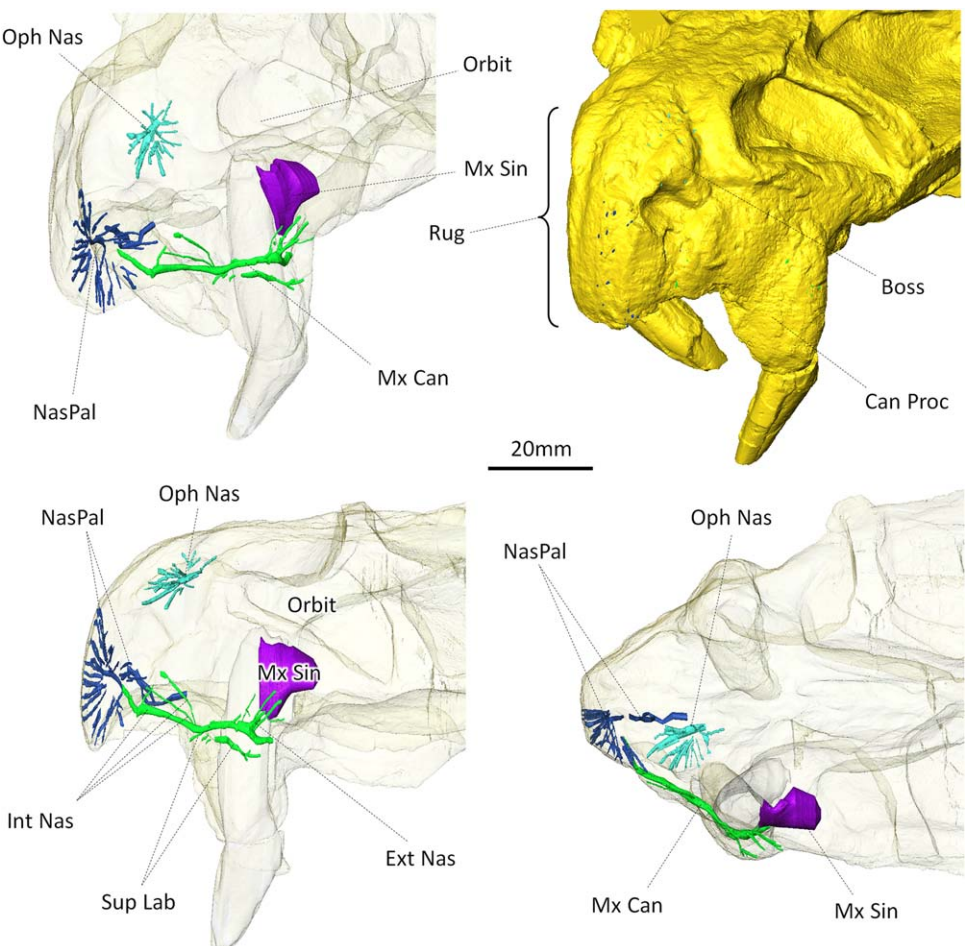


FIGURE 8 The trigeminal canals in *Diictodon feliceps* (SAM-PK-K11193). Top left, transparent skull in oblique view; Top right, solid skull in oblique view; Bottom left, lateral view; Bottom right, dorsal view. The ophthalmic canal is in light blue, the nasopalatine canal is in dark blue and the maxillary canal is in green. Abbreviations: Boss, nasal boss; Can Proc, caniniform process; Ext Nas, external nasal ramus; Int Nas, internal nasal ramus; Mx Can, maxillary canal; Mx Sin, maxillary sinus; NasPal, nasopalatine canal; Oph Nas, nasal ramus of the ophthalmic canal; Rug, rugosities of the ramphotheca; Sup Lab, superior labial ramus. Scale bar: 20 mm

area as the medial ramus (Figure 9). As in *Eodicyodon*, the maxillary sinus, which is located at the base of the zygomatic process, is occupied by the root of the tusk (Figure 7c).

Abajudon kaayai

Abajudon is an endothiodont dicynodont (Angielczyk et al., 2014a; Olroyd et al., in press) represented here by a skull (NHCC LB314) that is nearly complete aside from damage to the premaxilla and the anterior part of the maxilla. The specimen is far more complete than the holotype of *A. kaayai* described by Angielczyk et al. (2014a), and is referred to this species on the basis of its possession of the same highly distinctive maxillary teeth (see Olroyd et al. in press for details).

The ophthalmic canal is represented by both its frontal and nasal rami which are connected to each other by a deep antero-posteriorly oriented sulcus that excavates the endocranial face of the frontal and nasal bones (Figure 10). The nasal ramus appears much more ramified than the frontal ramus, and its ramifications are mostly oriented antero-posteriorly (Figure 10).

The nasopalatine canal is not preserved.

Despite the poor preservation of the rostrum, most of the maxillary canal can be described. The internal nasal ramus and the superior nasal ramus branch into numerous smaller canals that densely innervate and supply the rostral part of the maxilla laterally, and the region of the caniniform process, respectively (Figure 10). The external nasal ramus separates from the maxillary canal above the middle of the tooth row, not above the tusk as in other anomodonts (Figure 10). It is short and splits into one large branch directed dorsally, and three other smaller branches, a condition reminiscent of that in *Eodicyodon* (Figures 6, 10).

The alveolar rami are large and highly ramified, which likely reflects the large number of postcanine teeth (about ten) present in *Abajudon* (Figure 10). As in *Compsodon* and *Pristerodon* (see below), all alveolar rami originate from the maxillary sinus (Figure 10). The maxillary sinus itself is large because of the absence of the caniniform tooth (unlike in *Eodicyodon* and *Diictodon*) (Figure 7b), and it extends antero-posteriorly above the last five maxillary teeth (Figure 10). As in *Eodicyodon*, there is an ossified infraorbital canal that links the maxillary sinus to the orbital floor caudo-medially (Figure 10).

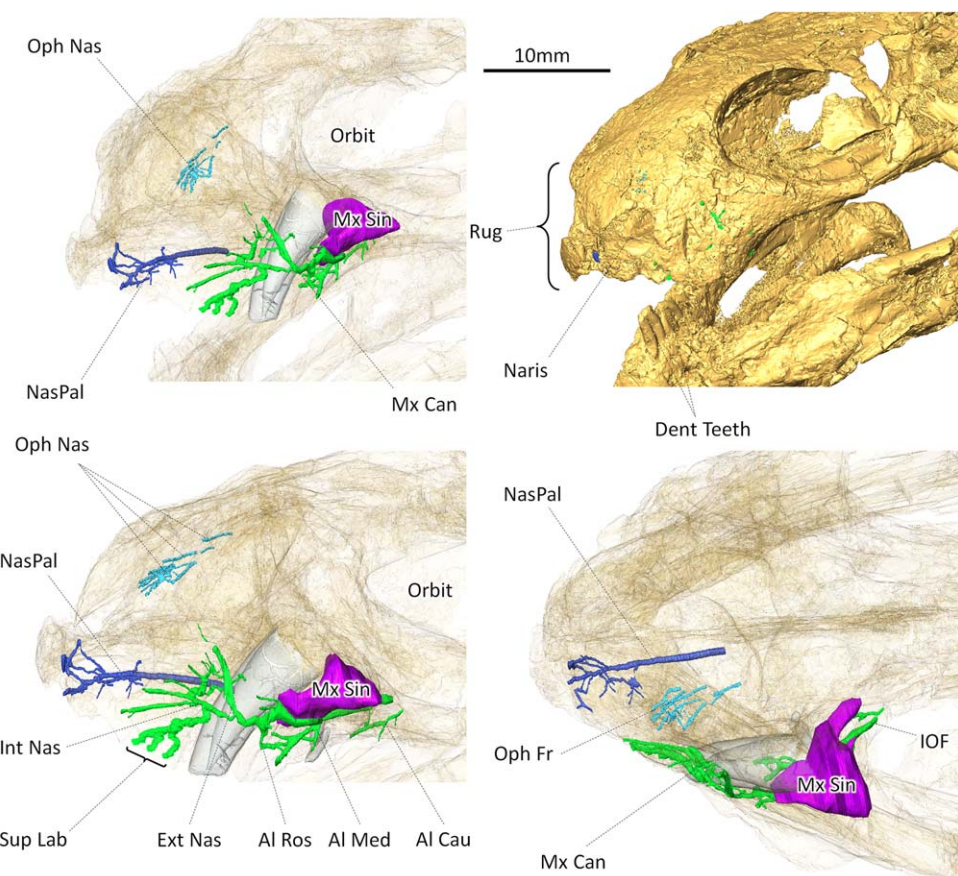


FIGURE 9 The trigeminal canals in *Pristerodon mackayi* (BP/1/2642). Top left, transparent skull in oblique view; Top right, solid skull in oblique view; Bottom left, lateral view; Bottom right, dorsal view. The ophthalmic canal is in light blue, the nasopalatine canal is in dark blue and the maxillary canal is in green. Abbreviations: Al Cau, caudal alveolar ramus; Al Med, medial alveolar ramus; Al Ros, rostral alveolar ramus; Dent Teeth, dentary teeth; Ext Nas, external nasal ramus; Int Nas, internal nasal ramus; IOF, infraorbital foramen; Mx Can, maxillary canal; Mx Sin, maxillary sinus; NasPal, nasopalatine canal; Oph Nas, nasal ramus of the ophthalmic canal; Rug, rugosities of the ramphotheca; Sup Lab, superior labial ramus. Scale bar: 10 mm

Compsodon helmoedi

Compsodon is an emydopodid dicynodont (Angielczyk et al., 2014b; Angielczyk & Kammerer, 2017) represented here by a complete skull (NHCC LB14). The spatial configuration of the trigeminal canals in *Compsodon* is similar to that in *Pristerodon*, but less ramified (Figure 11). The trigeminal canals end on the surface of the snout in areas bearing rugosity associated with the presence of the ramphotheca (Figure 11).

Only a small part of the nasal ramus of the ophthalmic canal is ossified (Figure 11). The canal is more or less parallel to the sagittal plane and gives off a few minor branches along its course.

There is a long, wide sulcus on the buccal surface of the palatal portion of the premaxilla for the nasopalatine nerve (Figure 11). As in *Pristerodon*, the nasopalatine canal starts at the postero-ventral margin of the premaxilla and ramifies rostrally into numerous smaller canals (Figure 11). Most ramifications open on the external surface of the beak, but some are oriented toward the buccal cavity (Figure 11).

The maxillary canal is only weakly ramified (Figure 11). The internal nasal ramus has three slender branches (Figure 11). One of them is directed to the palate and opens on the roof of the buccal cavity

(Figure 11). The other two open on the surface of the caniniform process (Figure 11). Unlike *Diictodon*, they do not extend beyond the level of the lateral margin of the naris (Figure 11). The superior labial ramus is located just ventral to the level of the external ramus and innervates and supplies the caniniform process (Figure 11). Unlike *Diictodon* and *Pristerodon*, the divergence points of the external and internal nasal rami are close to each other on the maxillary canal (Figure 11). As in *Eodicynodon*, the external nasal ramus is limited to only one branch, located dorsal to the tusk (Figure 11).

There are two short and non-ramified alveolar rami (Figure 11). They are both connected to the maxillary sinus. The more rostral branch goes to the area posterior to the tusk whereas the posterior branch goes to the area posterior to the two relictual postcanine teeth (Figure 11). They might represent the anterior and median alveolar rami, but based on the condition in *Pristerodon* (in which the median and posterior rami are connected to the maxillary sinus, but the anterior ramus is not) they are more likely to be the median and posterior branches. The maxillary sinus is occupied by the enlarged root of the tusk (Figure 11). There is no ossified infraorbital canal caudal to the maxillary sinus.

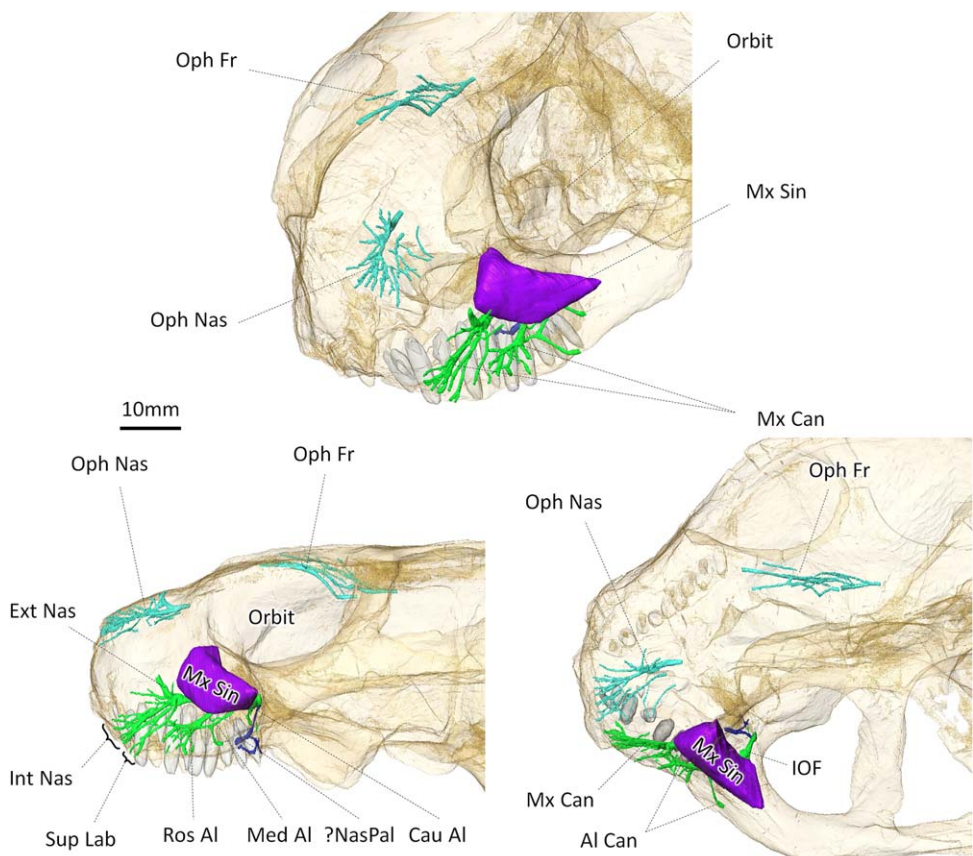


FIGURE 10 The trigeminal canals in *Abajudon kaayai* (NHCC LB314). Top, oblique view; Left, lateral view; right, dorsal view. The ophthalmic canal is in light blue, the possible root of the nasopalatine canal is in dark blue and the maxillary canal is in green. Abbreviations: Al Cau, caudal alveolar ramus; Al Med, medial alveolar ramus; Al Ros, rostral alveolar ramus; Ext Nas, external nasal ramus; Int Nas, internal nasal ramus; IOF, infraorbital foramen; Mx Can, maxillary canal; Mx Sin, maxillary sinus; NasPal, nasopalatine canal; Oph Fr, frontal ramus of the ophthalmic canal; Oph Nas, nasal ramus of the ophthalmic canal; Sup Lab, superior labial ramus. Scale bar: 10 mm

Myosaurus gracilis

Myosaurus is a peculiar genus of emydopodid dicynodont because it displays rugosity for the keratinous ramphotheca on the dentary only, but not on the maxilla and premaxilla (Cluver, 1974; Hammer & Cosgriff, 1981). This raises the possibility that the ramphotheca on the upper jaw was not as extensive in *Myosaurus* as was usually the case in dicynodonts (also see Surkov, 2006). In this study, *Myosaurus* is represented by four complete skulls (BP/1/2690; BP/1/2701a; BP/1/2701b; BP/1/4262). They all have a distinctive trigeminal canal morphology compared to other dicynodonts.

The nasal ramus of the ophthalmic canal is completely enclosed in *Myosaurus* and ramifies into numerous smaller branches (Figure 12). Since the premaxilla is antero-posteriorly short in *Myosaurus* (Cluver, 1974; Hammer & Cosgriff, 1981), the nasal ramus appears closer to the rostral margin of the skull in dorsal view than in other dicynodonts (Figure 12). The ramifications are mostly oriented antero-posteriorly and reach the posterior margin of the naris rostrally (Figure 12). A long and wide sulcus for the nasopalatine nerve is present on the buccal surface of the palatal portion of the premaxilla in all specimens except BP/1/2701a, in which the palate has been over-prepared (Figure 12). Nevertheless, BP/1/2701a is the only specimen that preserves the premaxilla anterior to the naris, and it demonstrates that the nasopalatine nerve

made only a minor contribution to the innervation and supply of the surface of the premaxilla, in a manner similar to non-anomodont therapsids (Figures 2–4, 12).

The maxillary canal is short and stubby in *Myosaurus* (Figure 12), and the extremities of its branches reach the surface of the maxilla at a comparatively long distance caudal to the naris (Figure 12). Rostrally, the three usual ramifications that comprise the maxillary canal—namely the internal nasal ramus, external nasal ramus and superior labial ramus—are anteroposteriorly short and barely recognizable (Figure 12). The external nasal ramus emits a long branch dorso-caudally which runs along the rostral margin of the maxillary antrum. In BP/1/2701a, the internal nasal ramus still maintains three distinct branches, as encountered in most NMS (Figures 2–4; Benoit et al., 2016a). There is no canine or caniniform process, but a small socket for a tusk is retained. Caudally, the maxillary canal passes through the maxillary antrum and its course can be followed to a discrete infraorbital foramen inside the orbit (Figure 12).

The number of alveolar rami is difficult to determine as there are a number of branches directed toward the ventral margin of the maxilla. These branches are particularly numerous in BP/1/2701b (Figure 12b). However, two branches are consistently present in all four specimens: one originating directly from the maxillary canal and another originating

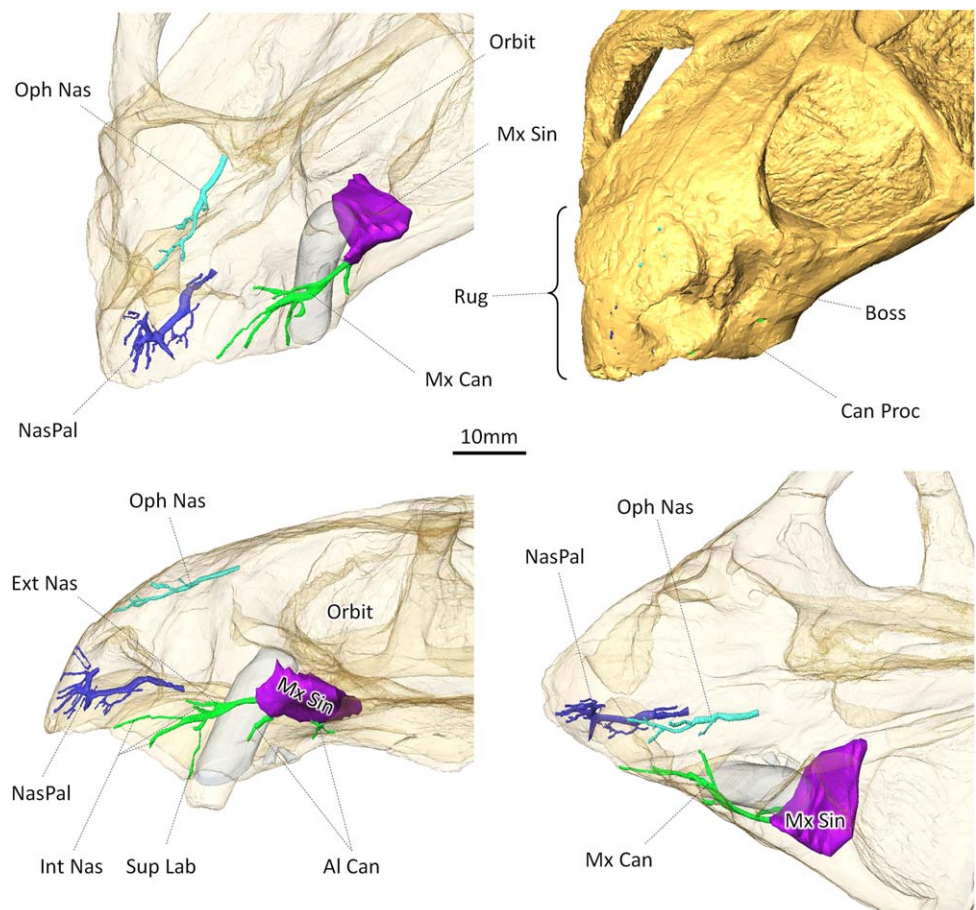


FIGURE 11 The trigeminal canals in *Compsodon helmoedi* (NHCC LB14). Top left, transparent skull in oblique view; Top right, solid skull in oblique view; Bottom left, lateral view; Bottom right, dorsal view. The ophthalmic canal is in light blue, the nasopalatine canal is in dark blue and the maxillary canal is in green. Abbreviations: Al Can, alveolar canals; Boss, nasal boss; Can Proc, caniniform process; Ext Nas, external nasal ramus; Int Nas, internal nasal ramus; Mx Can, maxillary canal; Mx Sin, maxillary sinus; NasPal, nasopalatine canal; Oph Nas, nasal ramus of the ophthalmic canal; Rug, rugosities of the ramphotheca; Sup Lab, superior labial ramus. Scale bar: 10 mm

from the maxillary antrum (Figure 12). They might correspond to the medial and caudal alveolar rami respectively, by analogy with *Compsodon*. There are no postcanine teeth.

The maxillary antrum (sinus) is located at the base of the zygomatic process, as is usual in dicynodonts. Because of the absence of tusks, the maxillary sinus is spacious and expansive both anteroposteriorly and mediolaterally (Figure 12).

Cistecephalidae

The description of the condition in cistecephalid dicynodonts is mostly based on the scan of a partial skeleton of a new cistecephalid from the Mid-Zambezi Basin (NHCC LB366) (Lungmus et al., 2015). The skull of this specimen is distorted, partly crushed, and the premaxillae are broken. Therefore, the description of the trigeminal canals is supplemented with that of the natural endocast of the ophthalmic canal preserved in a specimen of a second new cistecephalid species from the Luangwa Basin of Zambia (BP/1/3337; this taxon was briefly described by Angielczyk et al., 2014b). Additional literature is also used to complete this description, primarily Laaß and Kaestner's (2017) study of the maxillary canal in *Kawingasaurus fossilis* as well as the tomographic studies

of *Cistecephalus* by Keyser (1965, 1973) and Laaß and Schillinger (2015).

The ophthalmic canal is not ossified in NHCC LB366 (Figure 13), but the natural endocast preserved in BP/1/3337 distinctly shows that a sulcus for the ophthalmic nerve extends along the roof of the nasal cavity (Figure 13). This sulcus ramifies into three smaller branches rostrally, two of which diverge laterally (Figure 13). All three ramifications are located under the nasal bone and thus may be homologous to the nasal ramus. The pattern of foramina on NHCC LB366 (one foramen located caudally and several foramina located more rostrally) is consistent with the condition observed in BP/1/3337 (Figure 13).

The course of the nasopalatine canal is unclear in NHCC LB366 due to distortion and breakage at the level of the premaxilla. However, the presence of a ventro-medial canal ramifying in the proximal part of the premaxilla suggests that the beak was innervated and supplied by the nasopalatine canal as in other anomodonts (Figure 13). This is confirmed by the serial-grinding study of Keyser (1965: fig. 2) who figured a conspicuous canal running in the position of the nasopalatine canal in *Cistecephalus*. Pitting indicates that the ramphotheca was limited to the premaxilla and a small area dorsal to the nostril (Keyser, 1965).

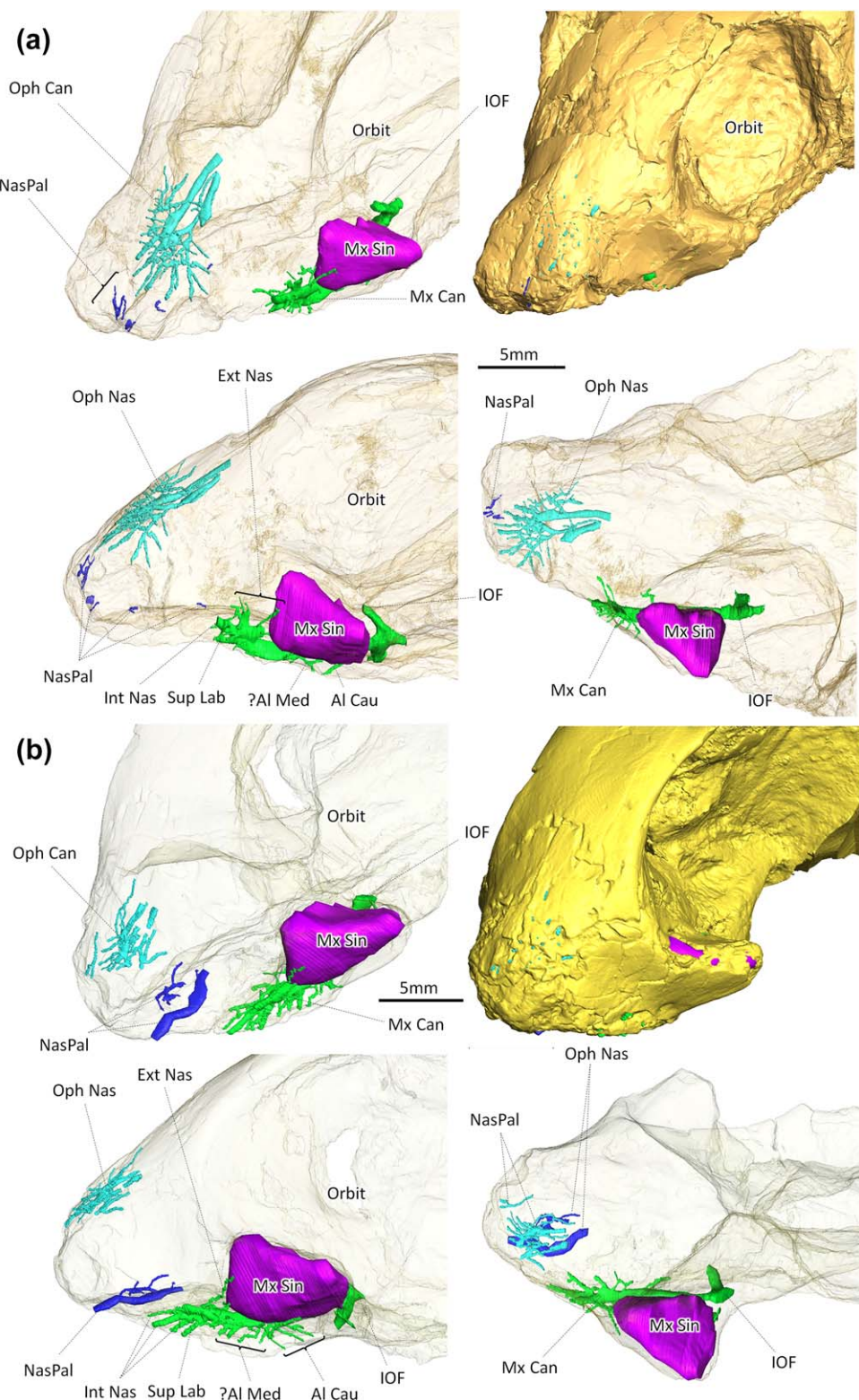


FIGURE 12 The trigeminal canals in *Myosaurus gracilis* (a BP/1/2701a; b BP/1/2701b). Top left, transparent skull in oblique view; Top right, solid skull in oblique view; Bottom left, lateral view; Bottom right, dorsal view. The ophthalmic canal is in light blue, the nasopalatine canal is in dark blue and the maxillary canal is in green. Abbreviations: Al Cau, caudal alveolar ramus; Al Med, medial alveolar ramus; Ext Nas, external nasal ramus; IOF, infraorbital foramen; Int Nas, internal nasal ramus; Mx Can, maxillary canal; Mx Sin, maxillary sinus; NasPal, nasopalatine canal; Oph Can, Ophthalmic canal; Oph Nas, nasal ramus of the ophthalmic canal; Rug, rugosities of the ramphotheca; Sup Lab, superior labial ramus. Scale bar: 5 mm

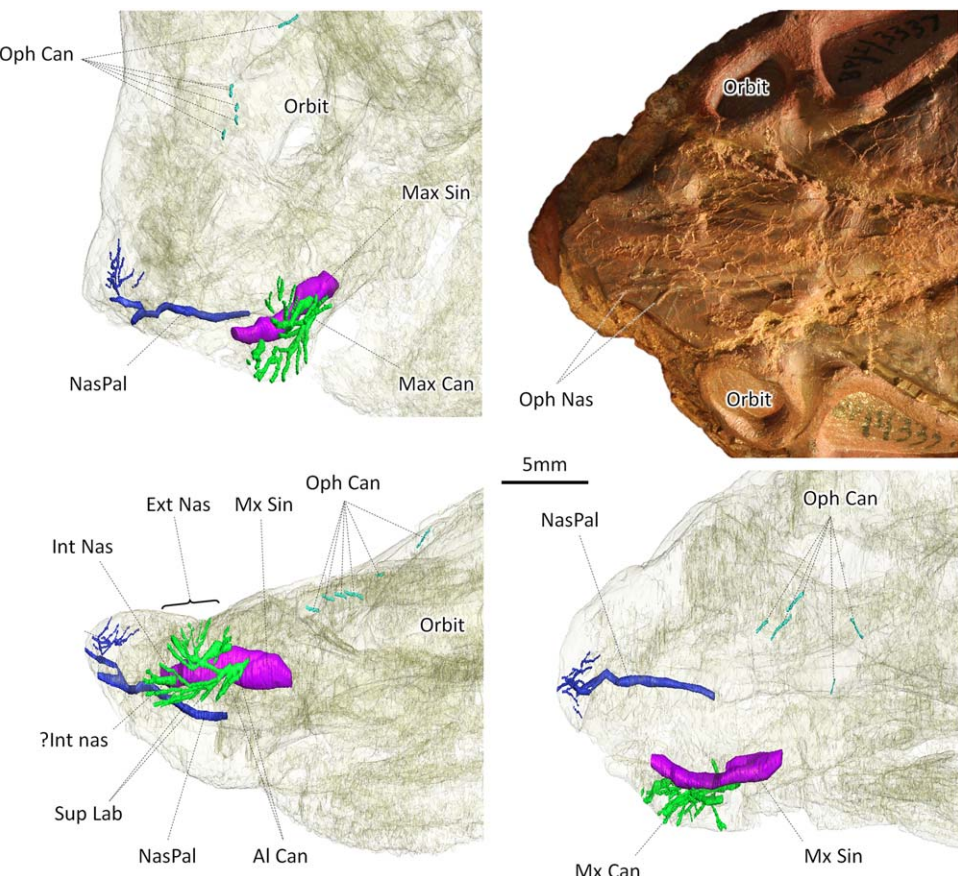


FIGURE 13 The trigeminal canals in *Cistecephalidae* gen. et sp. nov. (Mid-Zambezi Basin, Zambia) Top left, transparent skull (NHCC LB366) in oblique view; Top right, natural endocast of the ophthalmic canal in BP/1/3337 *Cistecephalidae* gen. et sp. nov. (Luangwa Basin, Zambia) in dorsal view; Bottom left, transparent skull of NHCC LB366 in lateral view; Bottom right, transparent skull of NHCC LB366 in dorsal view. The ophthalmic canal is in light blue, the nasopalatine canal is in dark blue and the maxillary canal is in green. Abbreviations: Al Can, alveolar canals; Boss, nasal boss; Ext Nas, external nasal ramus; Int Nas, internal nasal ramus; Mx Can, maxillary canal; Mx Sin, maxillary sinus; NasPal, nasopalatine canal; Oph Can, ophthalmic canal; Oph Nas, nasal ramus of the ophthalmic canal; Sup Lab, superior labial ramus. Scale bar: 5 mm. NHCC LB366 is mirrored for comparison

The maxillary canal in NHCC LB366 is poorly preserved, but our observations of this specimen (Figure 13) are complemented by the well preserved specimen of *Kawingasaurus* described by Laaß and Kaestner (2017). The internal nasal and superior labial rami in NHCC LB366 are highly ramified, as in *Pristerodon*, *Abajudon*, and *Eodicyndodon*. The superior labial ramus innervates and supplies the caniniform process whereas the internal nasal ramus goes to the rostro-ventral margin of the maxilla, lateral to the naris (Figure 13). In *Kawingasaurus*, these branches are similar in their branching pattern but are more strongly oriented antero-posteriorly (Laaß & Kaestner, 2017). The external nasal ramus is short and ramifies into numerous branches dorsally (Figure 13). In contrast, *Kawingasaurus* displays a short and un-ramified external nasal ramus (Laaß & Kaestner, 2017), which is consistent with the reconstruction of the maxillary canal of *Cistecephalus* made by Laaß and Schillinger (2015: fig. 4).

There are only two short, unbranched alveolar rami visible (Figure 13). Unlike *Compsodon*, they both originate from the maxillary canal (Figure 13). The maxillary sinus is antero-posteriorly extensive and spacious because of the absence of a tusk (Figure 13). An infraorbital foramen is present in *Kawingasaurus* (Laaß & Kaestner, 2017) but could not

be observed on NHCC LB366 because of preservation. In *Kawingasaurus*, there is only one short, unbranched alveolar ramus (Laaß & Kaestner, 2017). The reduction of the alveolar rami presumably coincides with the absence of postcanine-teeth in cistecephalids.

Oudenodon bainii

Oudenodon and *Lystrosaurus* represent the clade Bidentalalia in our dataset. This large clade also includes other cryptodonts such as *Tropidostoma*, *Aulacephalodon*, and *Pelanomodon*, basal dicynodontoids like *Dicynodon* and *Dapocephalus*, and the Triassic kannemeyeriforms (e.g., Kammerer & Angielczyk, 2009; Kammerer et al. 2011, 2013; Cox & Angielczyk, 2015; Angielczyk & Kammerer, 2017). As detailed below, the bidentalians in our dataset show important differences from other anomodonts in their pattern of trigeminal canal branching. *Oudenodon* is represented by a complete skull (NHCC LB631). As in other dicynodonts, the terminal openings of the trigeminal canals are located in the areas bearing rugosity associated with the ramphotheca (Figure 14).

Only the nasal ramus of the ophthalmic canal is ossified (Figure 14). This ramus is highly branched and innervates the surface of the

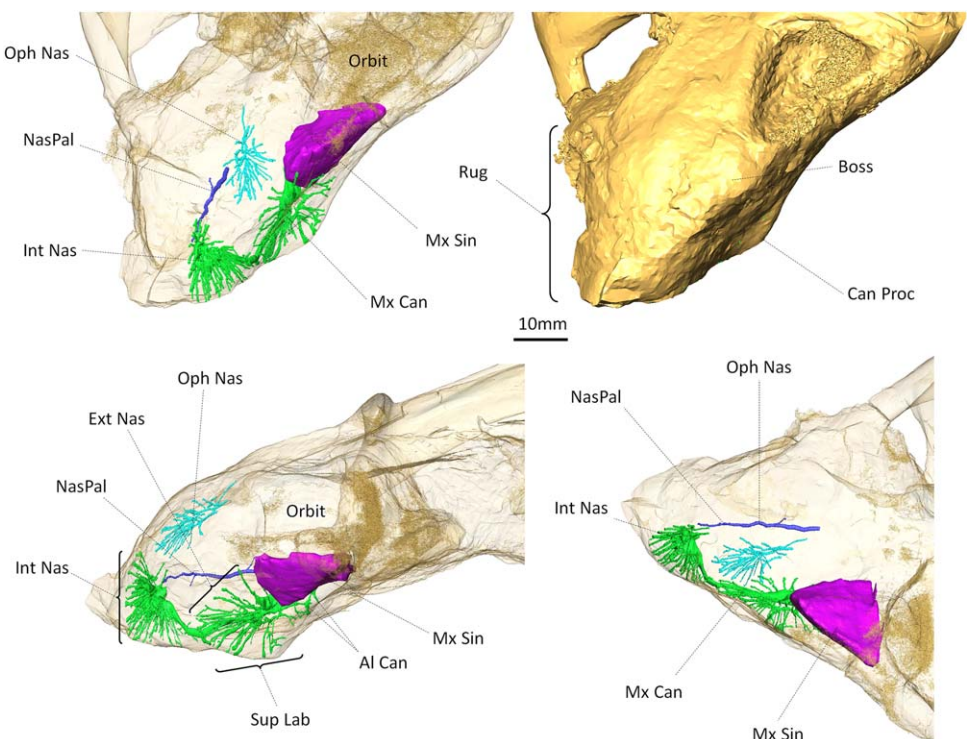


FIGURE 14 The trigeminal canals in *Oudenodon bainii*. Top left, transparent skull in oblique view; Top right, solid skull in oblique view; Bottom left, lateral view; Bottom right, dorsal view. The ophthalmic canal is in light blue, the nasopalatine canal is in dark blue and the maxillary canal is in green. Abbreviations: Al Can, alveolar canals; Boss, nasal boss; Can Proc, caniniform process; Ext Nas, external nasal ramus; Int Nas, internal nasal ramus; Mx Can, maxillary canal; Mx Sin, maxillary sinus; NasPal, nasopalatine canal; Oph Nas, nasal ramus of the ophthalmic canal; Rug, rugosities of the ramphotheca and frontal; Sup Lab, superior labial ramus. Scale bar: 10 mm

nasal bone (Figure 14). Rostrally, its ramifications extend to the caudal margin of the naris.

As in *Lystrosaurus* (see below), but unlike the other anomodonts in our dataset, the nasopalatine canal does not participate in the innervation and nutrition of the surface of the premaxilla. There is a long sulcus for the nasopalatine nerve which runs along the buccal surface of the palatal portion of the premaxilla, but the course of the nasopalatine canal ends in the trabeculae of the premaxilla, a few millimeters after the nerve has penetrated the bone (Figure 14). The morphology of the nasopalatine canal of *Oudenodon* differs from that of *Lystrosaurus* in not reaching the floor of the naris, which is instead innervated by the internal nasal branch of the maxillary canal (Figure 14).

All branches of the maxillary canal are highly ramified (Figure 14). Rostrally, the internal nasal ramus is extremely ramified and extends rostrally and medially beyond the level of the naris (Figure 14). As in *Lystrosaurus* (see below), it ramifies in the premaxilla, forming a large star-shaped plexus of branches directed toward the surface of the whole premaxilla, including the rostral part of its palatal portion (Figure 14). The internal nasal ramus is separated from the external nasal ramus by a long branch that gives off numerous, small ramifications ventrally (Figure 14). The superior labial ramus innervates and supplies the caniniform process with many ramifications (Figure 14), even though tusks are absent in *Oudenodon*. The external nasal ramus also is highly ramified, and emits numerous branches that ramify dorsal to the caniniform process (Figure 14).

Postcanine teeth are absent in *Oudenodon*, but there are two, reduced alveolar canals originating from the maxillary antrum (Figure 14), as in *Compsodon*, *Myosaurus*, and the Zambezi cistecephalid. The maxillary antrum is a wide and empty space because of the absence of a tusk (Figure 14). As in other dicynodonts, it extends into the base of the zygomatic process of the maxilla (Figure 14). There is no visible infraorbital foramen.

Lystrosaurus spp.

Two pristinely preserved, acid-prepared skulls, NMQR 815 (*L. declivis*) and NMQR 3595 (*L. curvatus*) were scanned and are described here. As in other dicynodonts, the terminal openings of the trigeminal canals are located at the external surfaces of the nasal, maxilla, and premaxilla in the areas bearing rugosity associated with the ramphotheca (Figure 15). In addition, the inter-orbital region is rugose in *Lystrosaurus* and likely had a keratinous covering (Grine, Forster, Cluver, & Georgi, 2006; Jasinoski & Chinsamy-Turan, 2012), and it is innervated by the frontal ramus of the ophthalmic canal (Figure 15).

In contrast to *Oudenodon*, both rami of the ophthalmic canal are ossified in *Lystrosaurus* (Figure 15). The frontal ramus ramifies inside the frontal bone and its numerous branches open onto the bone's interorbital surface (Figure 15). The nasal ramus innervates and supplies the surface of the nasal bone rostral to the orbit and its ramifications extend rostrally to reach the caudal margin of the naris (Figure 15). The

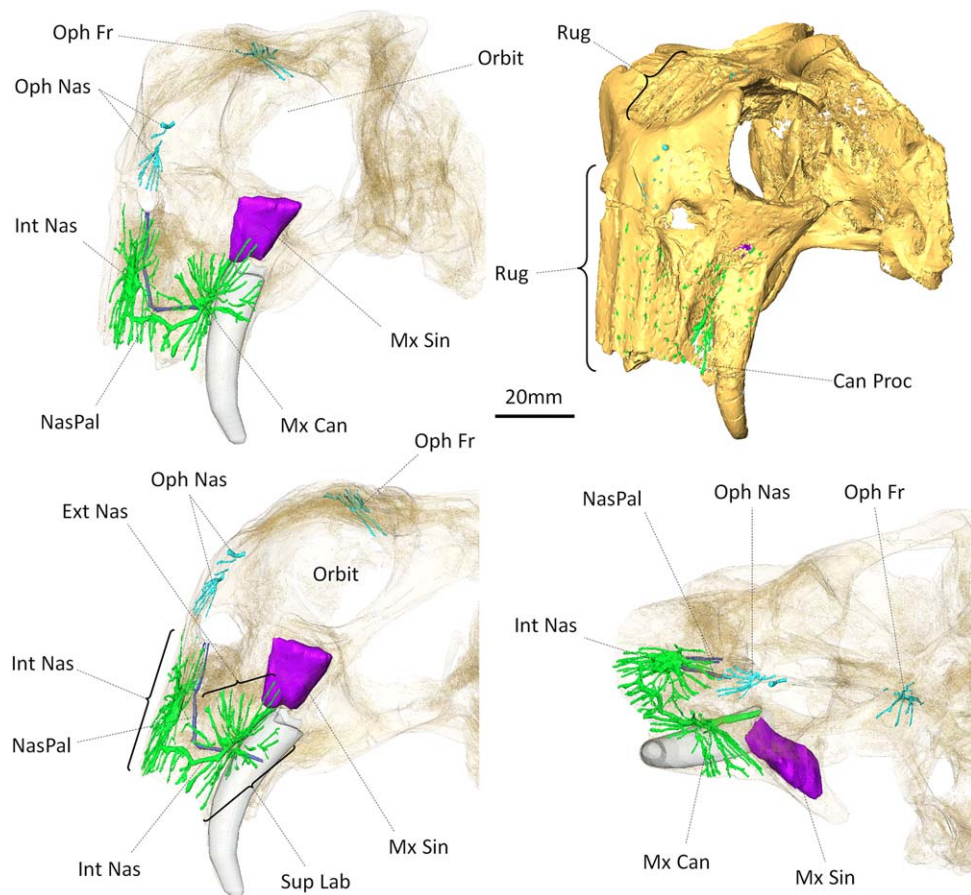


FIGURE 15 The trigeminal canals in *Lystrosaurus declivis* (NMQR 815). Top left, transparent skull in oblique view; Top right, solid skull in oblique view; Bottom left, lateral view; Bottom right, dorsal view. The ophthalmic canal is in light blue, the nasopalatine canal is in dark blue and the maxillary canal is in green. Abbreviations: Can Proc, caniniform process; Ext Nas, external nasal ramus; Int Nas, internal nasal ramus; Mx Can, maxillary canal; Mx Sin, maxillary sinus; NasPal, nasopalatine canal; Oph Fr, frontal ramus of the ophthalmic nerve; Oph Nas, nasal ramus of the ophthalmic canal; Rug, rugosities of the ramphotheca and frontal; Sup Lab, superior labial ramus. Scale bar: 20 mm

branches of the frontal ramus are oriented vertically, whereas those of the nasal ramus are oriented antero-posteriorly (Figure 15).

As in *Oudenodon*, the nasopalatine canal does not participate in the innervation and nutrition of the beak. There is a distinct sulcus for the nasopalatine nerve that runs along the buccal surface of the palatal portion of the premaxilla, as in other dicynodonts, but then it penetrates the nasopalatine canal at the ventral margin of the premaxilla, bends at a nearly 90° angle, and extends toward the naris (Figure 15). There, it emits two smaller canals that end on the floor of the naris (Figure 15). No anastomosis of the maxillary canal is visible in either of the *Lystrosaurus* specimens.

All branches of the maxillary canal are extremely ramified (Figure 15), similar to the condition in *Oudenodon*. Rostrally, the internal nasal ramus is the most ramified of all branches and the most modified compared to that of other NMS. As noted above, the nasopalatine canal no longer reaches the surface of the premaxilla, and is replaced by the internal nasal ramus (Figure 15). The internal nasal ramus extends rostrally and medially beyond the level of the naris (Figure 15). From here, it ramifies in every direction, forming a large star-shaped plexus of branches directed toward the surface of the whole premaxilla (Figure 15). This condition appears to be unique to bidentalians, as it is also

observed in *Oudenodon*. The external nasal ramus is also highly ramified, and it is separated from the internal nasal ramus by an elongated branch that itself gives off numerous, small ventral branches that innervate the anterolateral portion of the palatal rim (Figure 15). Unlike *Compsodon*, *Abajudon*, or *Eodicyndon*, the external nasal ramus of *Lystrosaurus* emits numerous branches that ramify dorsal to the tusk (Figure 15). The superior labial ramus also is highly ramified and reaches the surface of the caniniform process rostral to the canine (Figure 15).

There is no alveolar canal, consistent with the absence of postcanine teeth (Figure 15). The maxillary antrum is occupied by the large tusk root, and extends into the base of the zygomatic process of the maxilla (Figure 7d). Cluver (1971) also noted this posterior extension of the maxillary sinus in his detailed description of the skull of *Lystrosaurus*. There is no visible infraorbital foramen caudal to the maxillary antrum.

3 | DISCUSSION

3.1 | Character evolution in Anomodontia

To understand the evolutionary history of the trigeminal canals in anomodonts, we used parsimony to optimize a series of characters

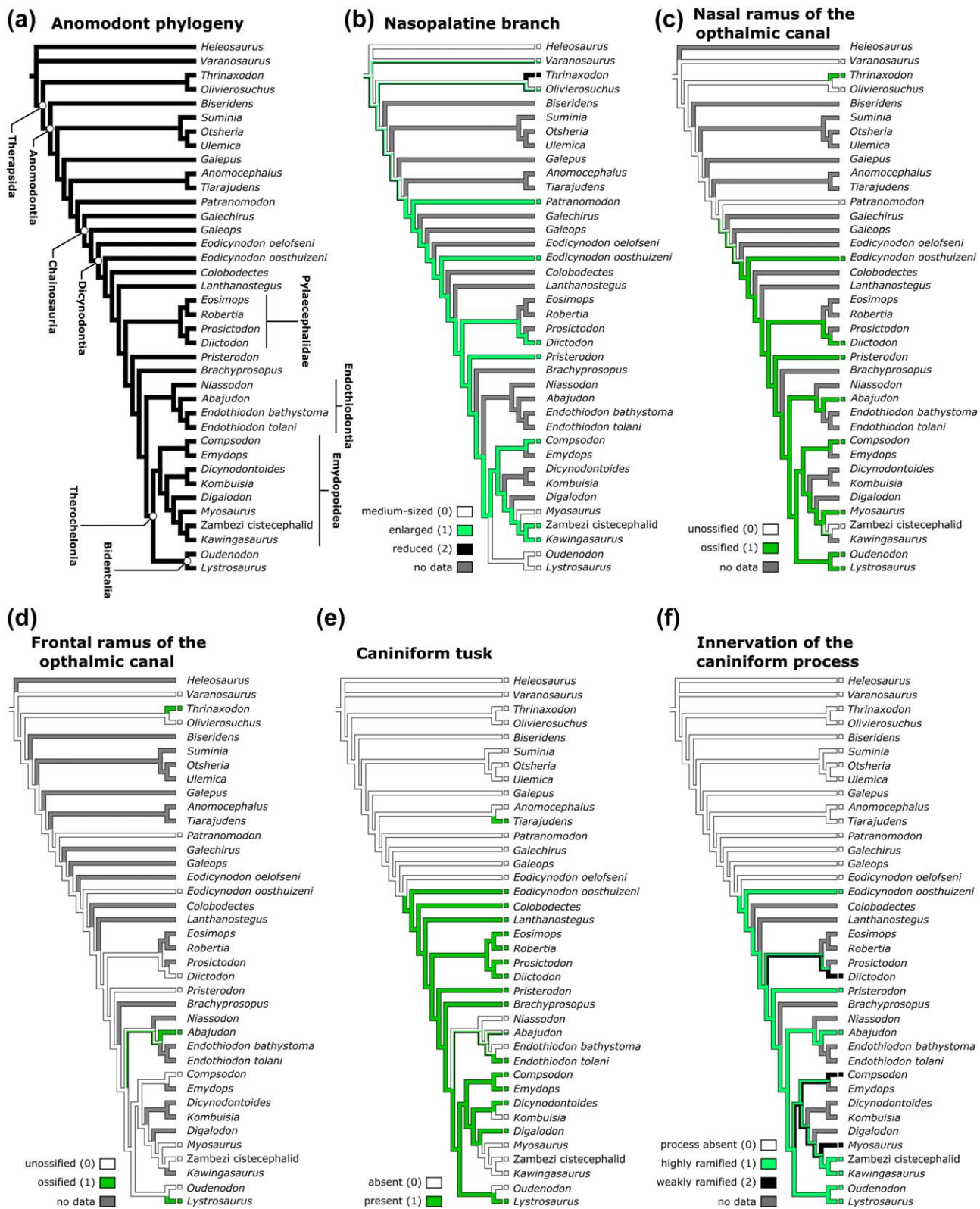
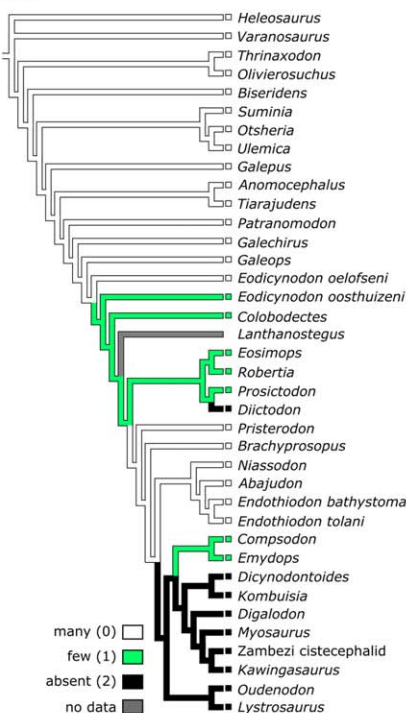


FIGURE 16 Results of the character state reconstructions. Phylogenetic tree after Angielczyk and Kammerer (2017). See the data matrix in Supplementary Information 1

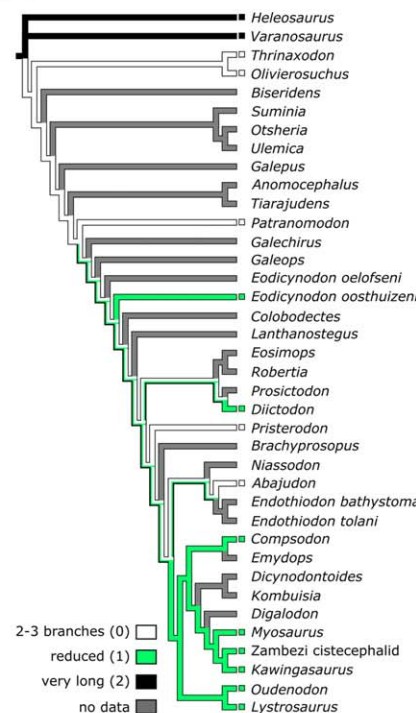
based on our data on a modified version of the tree presented in Angielczyk & Kammerer (2017). *Heleosaurus*, *Varanosaurus*, *Olivierosuchus*, and *Thrinaxodon*, as well as other taxa described in the literature

(Benoit et al., 2016a,b,2017a,b), were used to infer the ancestral internal anatomy, innervation, and supply of the snout that was present at the root of Anomodontia (Figure 16). Based on these taxa, the

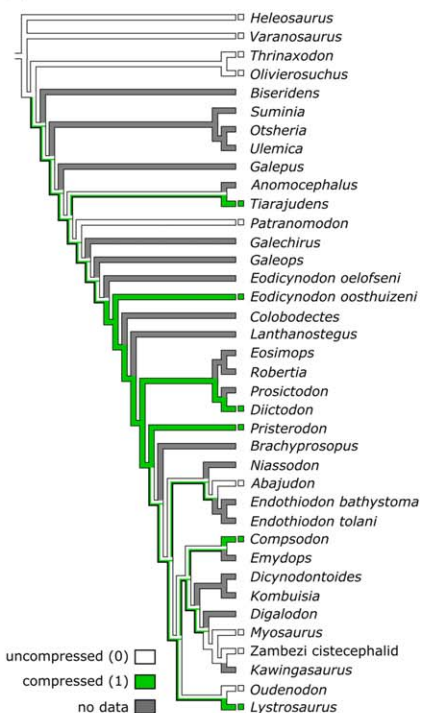
(g) Postcanine teeth



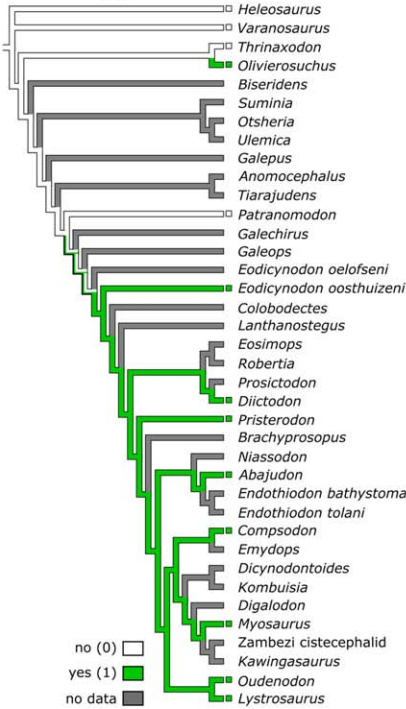
(h) Alveolar rami



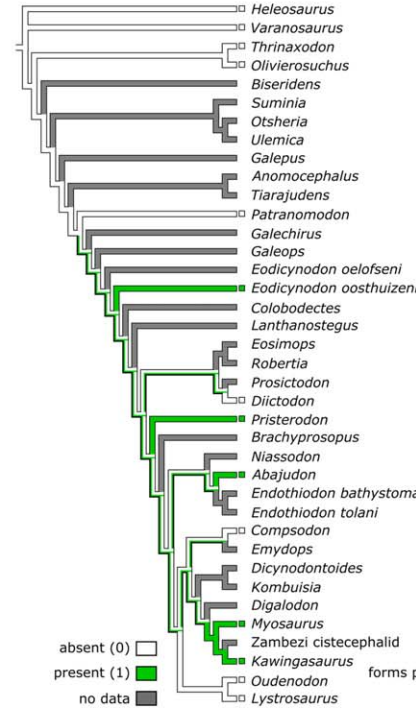
(i) Maxillary sinus



(j) Maxillary sinus extends into zygomatic process



(k) Infraorbital foramen



(l) Internal nasal ramus

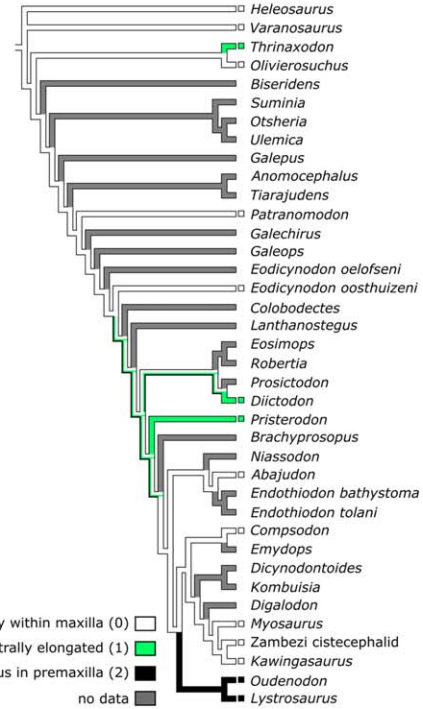


FIGURE 16 Continued

plesiomorphic condition includes: (a) a maxillary canal with three well-developed alveolar rami, the caudal-most ramus of which is extremely long in 'pelycosaurs' but not in therapsids (Figures 2–4, 16h); (b) the presence of three main rostral branches of the maxillary canal (the external and internal nasal rami, and the superior labial ramus), which

are themselves ramified into about three to six branches (Figures 2–4; Benoit et al. 2016a); (c) the presence of a maxillary sinus in which the maxillary canal vanishes caudally (Figures 2–4; Benoit et al. 2016a); (d) a short nasopalatine canal that contributes in part to the innervation of the premaxilla and leaves no sulcus on the buccal portion of the

premaxilla (in Eutheriodontia, the nasopalatine canal barely participates in the innervation of the premaxilla and may be connected to the internal nasal ramus, but this might constitute a secondarily-derived character) (Figure 16b); and potentially (e) an unossified ophthalmic canal (Figures 2, 16c, d; Benoit et al., 2016a, 2017a). Within the framework of this article, the first significant change in trigeminal canal anatomy related to anomodont evolution was the reduction of the caudal alveolar ramus near the base of Therapsida, which anomodonts subsequently inherited from their therapsid ancestors (Figure 16h).

3.2 | The origin of the ramphotheca in basal anomodonts

The oldest and most stemward non-dicynodont anomodont in our sample, *Patranomodon*, differs little from the ancestral condition except that it displays a well-defined sulcus on the buccal portion of the premaxilla that leads rostrally to a distinctly larger and more ramified nasopalatine canal (Figure 5). The clear sulcus left by the naso-palatine nerve and vessels, and the numerous ramifications of the canal in *Patranomodon*, suggest that the nasopalatine nerve and vessels were larger, more ramified, and assumed a more important role in the innervation and nutrition of the extremity of the premaxilla in non-dicynodont anomodonts than in other NMS. This condition is reconstructed as an unambiguous synapomorphy of the clade unifying *Patranomodon* with other, more derived anomodonts (although there is a reversal in Bidentalians; see below) (Figure 16b). Because *Varanosaurus* and *Oliverosuchus* display an intermediate condition in which the nasopalatine nerve ramifies in the premaxilla but leaves no deep sulcus on its buccal portion (which might be the plesiomorphic condition for NMS), the state of this character is reconstructed as ambiguous in anomodont taxa stemwards of *Patranomodon* (Figure 16b). Missing data for taxa such as the venyukovioids and anomocephaloids also contributes to the equivocal plesiomorphic state reconstruction for that portion of the tree, and investigation of these taxa would help to better pinpoint when the change occurred within Anomodontia. Finally, the exact optimization also depends on the phylogenetic placement of *Patranomodon* (e.g., it is reconstructed in a more stemward position in the analysis of Cox & Angielczyk, 2015, compared to the analyses of Angielczyk & Kammerer, 2017 and Angielczyk et al., in press, which would imply a deeper origin in Anomodontia).

The morphology of the nasopalatine canal in *Patranomodon* is reminiscent of that observed in chelonians, where the nasopalatine canal leaves a deep sulcus and abundantly innervates and supplies the surface of the premaxilla (Figure 1; Owen, 1866). This raises the possibility that at least a small ramphotheca covered the premaxilla in *Patranomodon*. The premaxilla is not preserved in the only specimen of *Patranomodon*, so it is impossible to assess whether rugosity associated with a ramphotheca was present. Such rugosity is absent in most other non-dicynodont anomodonts (*Biseridens*, *Anomocephalus*, *Tiarajudens*, venyukovioids, *Galechirus*), which display large premaxillary teeth instead of a beak (Brinkman, 1981; Ivakhnenko, 1996; Modesto & Rubidge, 2000; Liu et al., 2010; Cisneros, Abdala, Jashashvili, Bueno, & Dentzien-Dias, 2015). Brinkman (1981) suggested that an edentulous beak was

present in *Galeops* and *Galepus*, which is important given that *Galeops* typically is reconstructed as the sister taxon of Dicynodontia in most phylogenetic analyses (e.g., Kammerer et al., 2011, 2013; Cox & Angielczyk, 2015; Angielczyk & Kammerer, 2017). However, Brinkman's assessment of the character in *Galeops* was based on the holotype of *G. whaitsi* (AMNH FARB 5536); a natural mold in which the premaxilla is poorly preserved. Two more recently identified referred specimens of *G. whaitsi* (SAM-PK-4005, SAM-PK-12261) have better preserved premaxillae that clearly show that tooth alveoli were present on the premaxilla and that their seeming absence in the holotype is an artifact of preservation (Angielczyk, 2004). The only known skull of *Galepus* (AMNH FARB 5541) also is a natural mold, and although the anterior portion of the premaxilla appears to be edentulous, the preservation of the specimen and the presence of tooth impressions farther back on the jaws introduce some uncertainty as to whether the premaxilla originally was toothless. Even if a true beak did not evolve before the origin of dicynodonts, the chelonian-like enlargement of the nasopalatine canal in *Patranomodon*, where the roots of the premaxillary teeth are preserved, suggests that a transformation of the anatomy and sensitivity of the snout had already begun in basal anomodonts, which might have facilitated the evolution of the beak later in the clade's history.

The possible link between the anatomy of the nasopalatine canal and the presence of a ramphotheca is also supported by the data from *Myosaurus*. Unlike other dicynodonts, the upper jaw of *Myosaurus* displays no sign of the rugosity that marks the presence of a cornified cover (Cluver, 1974; Hammer & Cosgriff, 1981; Surkov, 2006). *Myosaurus* retains a long and deep sulcus for the nasopalatine nerve, but the portion of premaxilla preserved in BP/1/2701a shows that only a few ramifications actually reach the extremity of the snout (Figure 12a). The stubbiness of the maxillary canal, the retracted position of its rostral openings, and the variability of its morphology among specimens suggest that the trigeminal nerve was subject to weaker selective pressures in *Myosaurus* than in other dicynodonts, which is typical of biological structures that are no longer indispensable (see e.g., Benoit, Abdala, Van den Brandt, Manger, & Rubidge, 2015; Benoit et al., 2016a; Billet et al., 2012). These observations raise the possibility that the ramphotheca on the premaxilla of *Myosaurus* was reduced or absent (Surkov, 2006). Such reduction or loss would be surprising, considering that *Myosaurus* is edentulous and that there is evidence for a ramphotheca on the mandible (Cluver, 1974; Hammer & Cosgriff, 1981; Surkov, 2006). Further study of its sensory and feeding systems is clearly warranted.

3.3 | Character evolution at the root of Dicynodontia

The trigeminal canals of *Eodicynodon* and the other sampled dicynodonts differ extensively from the inferred ancestral condition found in the outgroups (Figure 16). For example, although a discrete infraorbital foramen for the CNV₂ located posterior to the maxillary sinus and which opens inside the orbit is reconstructed as an ambiguous dicynodont synapomorphy with reversals in *Diictodon*, *Compsodon*, and the bidentalians; Figure 16k), some of the ambiguity of this character is

likely the result of missing data. All of the dicynodonts, except the cistecephalids, also have an ossified nasal ramus of the ophthalmic canal, although the canal is ossified to varying degrees in different taxa (Figure 16c). The superior labial ramus is usually highly ramified in dicynodonts, except in *Compsodon*, *Diictodon*, and *Myosaurus*, and it supplies the caniniform process of the maxilla. (Figures 6, 8–15). This character is reconstructed as a synapomorphy of Dicynodontia, with the condition in *Diictodon*, *Compsodon*, and *Myosaurus* representing reversals (Figure 16f). Finally, with the exception of *Abajudon*, the cistecephalids, and *Oudenodon*, the sampled dicynodonts share the presence of an enlarged caniniform tusk in the maxilla (Figure 16e). The root of the tusk, when present, compresses the maxillary sinus and displaces it toward the zygomatic process of the maxilla, two characters that are reconstructed as synapomorphies of dicynodonts (Figure 16i, j).

Compression (or reduction in size) of the maxillary sinus is unequivocally reconstructed as the plesiomorphic state for dicynodonts (Figure 16i). Not surprisingly, this character state is correlated with the presence of the tusk: all of the tusked dicynodonts in our sample display the state, whereas tuskless taxa such as *Abajudon*, *Myosaurus*, the cistecephalids, and *Oudenodon* do not (Figure 16e, i). This observation is important for two reasons. First, in a strict parsimony framework, missing data for *Galechirus*, *Galeops*, and *Eodicynodon oelofseni* make the optimization for the character equivocal in the non-dicynodont chainosaurs, raising the possibility that these taxa had a compressed maxillary sinus. However, none of these taxa possessed a dicynodont-like tusk (or a distinct caniniform tooth at all), so it seems highly unlikely that their maxillary sinuses were reduced in size. Second, because caniniform tusks are ubiquitous among basal dicynodonts, and the absence of tusks in taxa such as the cistecephalids, *Myosaurus*, *Diictodon* and *Oudenodon* seem to represent secondary losses or polymorphism (e.g., *Abajudon*; see Sullivan, Reisz, & Smith, 2003; Olroyd et al., in press), we posit that the condition in these taxa are reversals associated with the loss of the tusk (Figure 16e, i). Notably, the non-dicynodont anomodont *Tiarajudens* has extremely enlarged, sabre-like caniniforms, and all phylogenies in which it has been included imply that its large caniniforms evolved independently from the tusks of dicynodonts (Cisneros, Abdala, Rubidge, Dentzien-Dias, & Bueno Ade, 2011; Cisneros et al., 2015). According to Cisneros et al. (2015:fig. 5), the maxillary sinus in *Tiarajudens* also was occupied by the root of the caniniform tooth, though the sinus seems to have been relatively spacious compared to the condition in dicynodonts when deformation is taken into account. This might be due to the extremely mediolaterally compressed shape of the caniniform in *Tiarajudens* compared to the more circular cross-section of the tusk root in dicynodonts. Assuming that the only known specimen of *Tiarajudens* accurately represents the morphology of the maxillary sinus lends further support to the hypothesis that the compressed maxillary sinus is a synapomorphy of dicynodonts associated with the evolution of the tusk in the clade.

In our current dataset, the presence of an ossified nasal ramus, resulting in the complete enclosure of the corresponding nerve inside the nasal bone, is reconstructed as an unambiguous synapomorphy of dicynodonts (Figure 16c). Apart from dicynodonts, this character has also been documented in *Thrinaxodon* and the dinocephalian *Moschos*

(Benoit et al. 2016a, 2017a), whereas the ramus is unossified in all other biarmosuchians, gorgonopsians, therocephalians, and non-mammalian cynodonts that have been examined to date (Benoit et al. 2016a,b). The lack of an ossified nasal ramus in *Patranomodon* and the seeming ubiquity of an unossified nasal ramus among NMS strongly suggest that this was the basal state for Anomodontia (Figure 16c). This could mean that the character state is a dicynodont synapomorphy, but missing data for *Galechirus*, *Galeops*, and *Eodicynodon oelofseni* raise the possibility that it also could have evolved on the dicynodont stem sometime after the divergence of *Patranomodon*. Further investigation of these taxa and other non-dicynodont anomodonts will be necessary to refine understanding of when in anomodont history an ossified nasal ramus of the ophthalmic canal evolved. It is possible that the nasal bone was covered by skin or a keratinous sheath that was involved in display for species recognition or intraspecific signaling (Benoit et al., 2016a). This would be consistent with the fact that the nasal ramus of the ophthalmic canal is more ramified in taxa with prominent nasal bosses such as *Eodicynodon*, *Diictodon*, *Compsodon*, and *Oudenodon* (Figures 6, 10, 11, 14).

3.4 | The effect of dentition on facial innervation

In addition to the morphology of the maxillary sinus noted above, two other characters seem to have been affected by the extensive transformation of the dentition that occurred in dicynodonts. The first of these characters is the reduction or loss of the alveolar rami of the maxillary canal. The alveolar rami of CNV₂ are responsible for innervating the tooth roots and surrounding regions (Rodella et al., 2012; Higashiyama & Kuratani, 2014). The ancestral state reconstruction for this character is equivocal from near the base of Chainosauria to the base of Therochelonia, where reduction of the alveolar ramus is unequivocally inferred to be the ancestral character state (Figure 16h). Part of this uncertainty stems from the large amount of missing data for basal dicynodonts, but it is also due to the complex pattern of evolution of the postcanine dentition of dicynodonts (Figure 16g).

All non-dicynodont anomodonts, apart from *Tiarajudens*, have an extensive postcanine dentition in the maxilla (Brinkman, 1981; Ivakhnenko, 1996; Rubidge & Hopson, 1996; Modesto & Rubidge, 2000; Rybcyzynski, 2000; Liu et al., 2010; Cisneros et al., 2015), and *Eodicynodon oelofseni* also retains three maxillary teeth (Rubidge, 1990a). In contrast, *Eodicynodon oosthuizeni*, *Colobodectes*, and ptyaecephalids other than *Diictodon* (in which postcanines are absent; e.g., Sullivan & Reisz, 2005) all retain only one to two relictual postcanines (e.g., Rubidge 1990b; Modesto, Rubidge, Visser, & Welman, 2003; Angielczyk & Rubidge, 2009, 2010, 2013). *Pristerodon*, *Brachyprosopus* and the endothiodonts have more extensive postcanine dentitions (e.g., Keyser, 1993; Castanhinha et al., 2013; Angielczyk et al., 2014a; Cox & Angielczyk, 2015), which parsimony reconstructs as a reversal to the basal character state (Figure 16g). Finally, absence of a postcanine dentition is reconstructed as the plesiomorphic state for Therochelonia, with secondary reversals to the presence of a small number of postcanines in *Emydops* and *Compsodon* (Figure 16g). Our data indicate that there is only a general correlation between the loss of postcanines and

the reduction of the alveolar rami (Figure 16g, h). For example, in *Eodicynodon oosthuizeni* the alveolar ramus is completely lost (Figure 6), despite the retention of a small number of postcanines, whereas the alveolar rami are reduced but not completely lost in the cistecephalids and *Oudenodon* (Figure 13), which retain no postcanine dentition. Because of this complexity we cannot definitively resolve the evolutionary history of the alveolar rami in dicynodonts without more detailed sampling of basal dicynodonts.

The second character is the pattern of innervation of the maxilla, particularly the caniniform process, by the superior labial ramus. In all of the sampled dicynodonts except *Diictodon*, *Compsodon*, and *Myosaurus*, the superior labial ramus is moderately to highly ramified, richly supplying the caniniform process of the maxilla. Extensive ramification of the superior labial ramus is reconstructed as a synapomorphy of dicynodonts in our dataset, and this is also the node where the tusk and caniniform process of the maxilla first appear (Figure 16e, f). As the caniniform process houses the tusk, the association between these structures is clear, and there are few cases among dicynodonts, such as *Endothiodon tolani*, where the tusk is present but a well-developed caniniform process is absent. It follows that as these structures were being elaborated, the superior labial ramus would also increase in complexity. Reduction of the postcanine dentition and evolution of the keratinous beak also might have been important here. For example, in addition to representing the phylogenetically earliest instance of the presence of a tusk and caniniform process, *Eodicynodon oosthuizeni* also shows good evidence for the presence of a beak and has a highly reduced postcanine dentition. Given the general relationship between reduction of the alveolar rami and reduction of the postcanines noted above, it is unsurprising that the superior labial ramus would take over innervation of the anterior regions of the maxilla as the alveolar rami were being reduced. However, as is the case with the correlation between the presence of postcanines and the morphology of the alveolar rami, the elaboration of the superior labial ramus is not precisely associated with the presence of the caniniform process and tusk (Figure 16e, f). For example, *Compsodon* and *Diictodon* have simplified superior labial rami, despite possessing both the tusk and caniniform process (Figures 10, 11). The case of *Diictodon* is especially puzzling given that the caniniform process appears to have played a key role in its feeding system (e.g., Cluver, 1970; Hotton, 1986; Rayner, 1992; Cox, 1998; Cox & Angielczyk, 2015). Study of additional taxa will be necessary to determine whether the condition in *Diictodon* is an autapomorphic reversal or perhaps a more general ptylaecephalic synapomorphy, and to better understand the evolution of the superior labial ramus in emydopoids (i.e., do the reductions in *Compsodon* and *Myosaurus* represent independent reversals or did cistecephalids re-elaborate the ramus, perhaps as part of the transition to a fossorial lifestyle?).

3.5 | General overview and significance for anomodont evolution

In summary, the results of our examination of the evolution of the trigeminal canals in anomodonts fit well with apparent evolutionary patterns related to the loss of the postcanine dentition and the evolution

of the beak in the clade. A major evolutionary transition occurred at the base of Dicynodontia, with the appearance of an extensive secondary palate, significant reduction in the dentition (i.e., loss of premaxillary teeth and retention of only a small number of maxillary postcanines), and the gain of a keratinous beak. Even the basal dicynodont *Eodicynodon oosthuizeni* is far more similar to later dicynodonts in these characters than to non-dicynodont chainosaurs such as *Galeops* (c.f., the positions of *Galeops* and *E. oosthuizeni* in the morphospace of Ruta et al., 2013), despite retaining some pleiomorphic character states in other parts of the skull (Barry, 1974; Rubidge, 1984, 1990b; King et al., 1989).

These changes in cranial morphology appear to have been accompanied by changes in the trigeminal canals and associated structures that are optimized as occurring at the base of Dicynodontia (i.e., reduction of the maxillary sinus, ossified nasal ramus of the ophthalmic canal, reduction of the alveolar rami of the maxillary canal, elaboration of the superior labial ramus in the vicinity of the caniniform process), although it is interesting to note that at least one important change—enlargement and increased ramification of the nasopalatine canal—occurred before the evolution of the beak (Figure 16b). Once the basic ground plan for the dicynodont skull was established, experimentation continued in the clade, including changes in the details of the secondary palate and variation in the number of postcanine teeth. This was accompanied by additional changes to the trigeminal canals, and there is evidence, such as the varying degrees of reduction of the alveolar branches observed in our sampled taxa, to suggest that some of these changes occurred homoplastically (Figure 16). The beaks and innervation patterns of bidentalians dicynodonts tend to display more consistency in morphology and structure than is the case for the more stemward taxa that we focused on here (Figures 14–16). For example, there is considerable variation in the presence and number of postcanine teeth in non-bidentalians, whereas only a handful of bidentalians such as *Tropidosotma*, *Australobarbarus*, and *Rastodon* retain postcanines (Kurkin, 2000; Botha & Angielczyk, 2007; Boos, Kammerer, Schultz, Soares, & Ilha, 2016). Because of this, we predict that bidentalians examined in the future will present similar morphologies. However, the bidentalians studied here display some novel character states indicating that the evolution of facial innervation did not stop completely at the base of Bidentalalia (Figure 16).

Indeed, bidentalians have undergone a significant reorganization of the trigeminal canals compared to the other dicynodonts included in this study, which implies that their pattern of facial innervation also was different. The nasopalatine ramus no longer innervates the rostral end of the premaxilla (Figure 16b). In *Lystrosaurus*, it now primarily supplies the area around the external naris, whereas in *Oudenodon*, it simply vanishes inside the premaxilla (Figures 14, 15). In its place, the highly ramified internal nasal ramus innervates the rostral end of the premaxilla. In both bidentalians examined here, this branch originates in the maxilla and extends rostrally to the premaxilla through a long canal that emits ventral ramifications along the margin of the upper jaw (Figures 14, 15). Once inside the premaxilla, it forms a large plexus that sends ramifications in all directions (Figures 14, 15). This morphology is unique to bidentalians, and given that *Oudenodon* and *Lystrosaurus* are

distant relatives within this clade (Angielczyk & Kammerer, 2017), it is likely a conserved synapomorphy of Bidentalians (Figure 16l). The portions of the external nasal ramus and superior labial ramus that supply the rest of the palatal rim and caniniform process are ramified to an unusual degree as well (Figures 14, 15).

Besides the unusual arrangement of the trigeminal canals, the degree of ramification of the nerves innervating the surface of the snout in bidentalians is also striking. This suggests that the snout of bidentalians was more sensitive than in the other taxa we examined, although the need for this increased sensitivity is unclear. *Lystrosaurus* frequently has been suggested to have had an amphibious, hippopotamus-like ecology (Broom 1903a, b, 1932; Watson, 1912, 1913; Brink, 1951; Camp, 1956; Cluver, 1971; Kemp, 1982; Hotton, 1986; Germain & Laurin, 2005; Ray et al., 2005; Canoville & Laurin, 2010; although see King, 1991; King & Cluver, 1991; Botha & Smith, 2007; Botha-Brink & Angielczyk, 2010), and the ventrally extended snout has been suggested to be an adaptation to allow it to feed with the face partially submerged. If this is correct, then receptors connected to the trigeminal nerve, such as tactile receptors similar to the dome pressure receptors present on the snout of crocodilians (Leitch & Catania, 2012) or electroreceptors similar to those of monotremes (Manger & Pettigrew, 1995, 1996) may have been present. The presence of similar receptors has already been hypothesized in a wide variety of therapsids including the Russian therocephalian *Perplexisaurus* (Tatarinov, 1999; Ivakhnenko, 2001; Surkov, 2006). Alternatively, the arrangement of the jaw musculature, construction of the skull, and the presence of a patent suture between the premaxilla and maxilla all suggest that *Lystrosaurus* had a powerful, snapping bite (Crompton & Hotton, 1967; Cluver, 1971; Jasinoski, Rayfield, & Chinsamy, 2009, 2010a, 2010b), and increased innervation of the snout may have increased food selectivity during feeding, as recently hypothesized in dinosaurs (Barker et al., 2017). Both of these hypotheses, however, do not account for the presence of a similar ramification pattern in *Oudenodon*, which is generally regarded as terrestrial and having a less specialized feeding system and mechanical properties of the skull (Jasinoski et al. 2009, 2010a, b). Finally, there is evidence that *Oudenodon* and *Lystrosaurus* spent time in burrows (e.g., Groenewald, 1991; Botha, 2003; Modesto & Botha-Brink, 2010; Krapovickas, Mancuso, Marsicano, Domnanovich, & Schultz, 2013; Botha-Brink, 2017), and the other burrowing dicynodonts included in our dataset (*Diictodon* and the cistecephalids) have highly innervated regions of their snouts as well (Figures 10, 13; Laaß & Kaestner, 2017). This may indicate that tactile reception from the face was an important source of sensory input for dicynodonts when underground.

Interestingly, despite occupying a disparate phylogenetic position, the burrowing taxon *Diictodon* displays some characters of the trigeminal canals that are reminiscent of bidentalians. The internal nasal ramus of *Diictodon* not only innervates the maxilla, but also extends rostrally to reach the surface of the premaxilla, as in bidentalians (Figure 10). The divergence points of the external and internal nasal rami also are separated by a long segment of the maxillary canal only in *Diictodon*, *Oudenodon*, and *Lystrosaurus* in our dataset (Figures 10, 14, 15). However, there are also important differences between these taxa. For

example, the nasopalatine canal only sends a few branches to the interior of the naris in *Lystrosaurus* (Figure 15), unlike *Diictodon* in which the premaxilla is still mostly innervated and supplied by the nasopalatine canal (Figure 10). Given these differences, and the large number of other characters that suggest that *Diictodon* is distantly related to Bidentalians, it is almost certain that the similarities of the internal and external nasal rami are homoplasies (Figure 16l), perhaps related to burrowing habits.

3.6 | Facial innervation and skull shape evolution in *Lystrosaurus*

The trigeminal canal anatomy of *Lystrosaurus* is intriguing when considered in the context of the unusual skull shape of the taxon compared to other dicynodonts. Since the earliest descriptions of specimens now recognized as representing *Lystrosaurus* (Huxley, 1859; Owen, 1860), authors have commented on the unusual deepening of the snout. Cluver (1971) considered the proportional changes in the snout of *Lystrosaurus* in detail. He found that compared to more "normally" proportioned dicynodonts, the nostril of *Lystrosaurus* is in roughly the same position relative to the basicranial axis, whereas the palatal rim has been shifted ventrally. The mechanism effecting this change primarily appears to be the ventral extension of the premaxilla, with concomitant morphological changes in other elements, such as deepening of the vomerine septum.

A logical scenario for the evolution of the facial innervation in *Lystrosaurus* follows from Cluver's (1971) proposed mechanism for the deepening of the snout in this taxon (ventral lengthening of the subnarial portion of the premaxilla) and the anatomy of the trigeminal canals observed here. In the other dicynodonts examined in this study, the nasopalatine canal (and associated nerve) runs along the roof of the buccal cavity, passing close to the external naris, and ramifies to innervate the rostral portion of the premaxilla (Figures 5–13). In *Lystrosaurus*, the nasopalatine canal also passes along the dorsal surface of the buccal cavity before sharply bending and innervating the area near the external naris (but not the rostral surface of the premaxilla) (Figure 15). This suggests that the nasopalatine canal was forced to maintain its ancestral association with the external naris as the subnarial portion of the premaxilla extended ventrally. Moreover, the snout deepening in *Lystrosaurus* may have been facilitated further by the replacement of the nasopalatine ramus by the internal nasal ramus of the maxillary canal as the main source of innervation of the premaxilla in Bidentalians, which freed the nasopalatine ramus from having to maintain an association with the alveolar region of the premaxilla (Figure 15).

Although this scenario is speculative, it likely can be tested. Recent phylogenetic analyses have consistently reconstructed the Permian dicynodonts *Eptychognathus bathyrhynchus* and *Kwazulusaurus shakai* (if it is a valid taxon) as members of Lystrosauridae, and *Sintocephalus alticeps*, *Basilodon woodwardi*, and *Syops vanhoepeni* are also sometimes considered members of this clade (Kammerer et al., 2011, 2013; Castanhinha et al., 2013; Cox & Angielczyk, 2015; Boos et al., 2016; Angielczyk et al., in press). These taxa have less extreme snout morphologies than *Lystrosaurus* and might preserve intermediate

arrangements of the trigeminal canals that could elucidate the details of the transition.

4 | CONCLUSION

Anomodonts are distinguished from all other NMS by the greater importance of the nasopalatine nerve in the innervation of the snout. This condition is similar to that encountered in turtles, suggesting that it is likely correlated with the evolution of the beak in both clades. Here we highlight a complex series of transformations, with multiple homoplastic losses of the alveolar rami and reduction of the maxillary sinus correlated to the numerous reductions, losses and potential re-acquisitions of the postcanine dentition and tusk. Despite this, some trends can be traced. It appears that the trigeminal canals evolved under the strong influence of both the dentition and the ramphotheca. Taxa with reduced or absent postcanine teeth are more likely to lose their alveolar rami, and taxa with large tusks have a compressed maxillary antrum. In this respect, the typical dicynodont condition (large tusk, small maxillary antrum, no premaxillary and postcanine teeth, alveolar ramus absent) was already achieved in *Eodicynodon* and then, with some degree of convergence, in many other more derived taxa. The evolution of the trigeminal canals and sensitivity in dicynodonts highlight another example of the complexity of dicynodont evolution. This underscores the fact that the extensive radiation of dicynodonts produced a tremendous diversity of forms and functional types, and that they deserve special attention among NMS.

ACKNOWLEDGMENTS

We thank the following institutions for access to specimens: the American Museum of Natural History (New York City, U.S.A.), the Evolutionary Studies Institute (Johannesburg, South Africa), the Council for Geoscience (Pretoria, South Africa), the Field Museum of Natural History (Chicago, U.S.A.), the National Heritage Conservation Commission (Lusaka, Zambia), the National Museum (Bloemfontein, South Africa), and the Iziko Museum of Natural History South Africa (Cape Town, South Africa). We acknowledge the European Synchrotron Radiation Facility for provision of synchrotron radiation facilities, and we would like to thank P. Tafforeau for assistance in using beamline ID17. J. Lungmus assisted with data collection that University of Chicago PaleoCT facility. This research was conducted with financial support from the Claude Leon Foundation; PAST and its scatterlings projects; the NRF African Origin Platform; and the DST-NRF Centre of Excellence in Palaeosciences (CoE in Palaeosciences). Opinions expressed and conclusions arrived at, are those of the authors and are not necessarily to be attributed to the CoE in Paleosciences.

CONFLICT OF INTEREST

The authors declare no competing interests.

AUTHOR CONTRIBUTIONS

Study concept and design: JB, KDA. Acquisition of data: JB, KDA, JAM, VF. Analysis and interpretation of data: JB, KDA. Drafting of the manuscript: JB, KDA. Critical revision of the manuscript for important intellectual content: JAM, PM, VF, BR. Obtained funding: JB, PM, BR. Administrative, technical, and material support: PM, BR. Study supervision: PM, BR. All authors gave final approval for publication.

ORCID

Julien Benoit  <http://orcid.org/0000-0001-5378-3940>

Paul Manger  <http://orcid.org/0000-0002-1881-2854>

REFERENCES

- Abdel-Kader, T. G., Ali, R. S., & Ibrahim, N. M. (2011). The Cranial Nerves of *Mabuya quinquaeniata* III: Nervus Trigeminus. *Life Science Journal*, 8, 650–669.
- Angielczyk, K. D. (2004). Phylogenetic evidence for and implications of a dual origin of propaliny in anomodont therapsids (Synapsida). *Paleobiology*, 30(2), 268–296.
- Angielczyk, K. D., Hancox, P. J., & Nabavizadeh, A. (In Press). A redescription of the Triassic kannemeyeriform dicynodont *Sangsaurus* (Therapsida, Anomodontia), with an analysis of its feeding system. In C. A. Sidor, & S. J. Nesbitt, (eds.), *Vertebrate and Climatic Evolution in the Triassic Rift Basins of Tanzania and Zambia*. Society of Vertebrate Paleontology Memoir 17. *Journal of Vertebrate Paleontology* 37 (6, Supplement).
- Angielczyk, K. D., Huertas, S., Smith, R. M. H., Tabor, N. J., Sidor, C. A., Steyer, J.-S., ... Gostling, N. J. (2014a). New dicynodonts (Therapsida, Anomodontia) and updated tetrapod stratigraphy of the Permian Ruhuhu Formation (Songea Group, Ruhuhu Basin) of southern Tanzania. *Journal of Vertebrate Paleontology*, 34, 1408–1426.
- Angielczyk, K. D., & Kammerer, C. F. (2017). The cranial morphology, phylogenetic position, and biogeography of the upper Permian dicynodont *Compsodon helmoedi* van Hoepen (Therapsida, Anomodontia). *Papers in Palaeontology*, 3, 513–545.
- Angielczyk, K. D., & Rubidge, B. S. (2009). The Permian dicynodont *Colobodectes cluveri* (Therapsida, Anomodontia), with notes on its ontogeny and stratigraphic range in the Karoo Basin, South Africa. *Journal of Vertebrate Paleontology*, 29, 1162–1173.
- Angielczyk, K. D., Rubidge, B. S., Day, M. O., & Lin, F. (2016). A reevaluation of *Brachypterus broomi* and *Chelydopterus altidentalis*, dicynodonts (Therapsida, Anomodontia) from the middle Permian *Tapinocephalus* Assemblage Zone of the Karoo Basin, South Africa. *Journal of Vertebrate Paleontology*, 36(2), e1078342.
- Angielczyk, K. D., & Rubidge, B. S. (2010). A new ptylaecephalid dicynodont (Therapsida, Anomodontia) from the *Tapinocephalus* Assemblage Zone, Karoo Basin, Middle Permian of South Africa. *Journal of Vertebrate Paleontology*, 30, 1396–1409.
- Angielczyk, K. D., & Rubidge, B. S. (2013). Skeletal morphology, phylogenetic relationships and stratigraphic range of *Eosimops newtoni* Broom, 1921, a ptylaecephalid dicynodonts (Therapsida, Anomodontia) from the Middle Permian of South Africa. *Journal of Systematic Palaeontology*, 11(2), 191–231.
- Angielczyk, K. D., Steyer, J.-S., Sidor, C. A., Smith, R. M. H., Whatley, R. L., & Tolan, S. (2014b). Permian and Triassic dicynodont (Therapsida: Anomodontia) faunas of the Luangwa Basin, Zambia: Taxonomic update and implications for dicynodont biogeography and

- biostratigraphy. In C. F. Kammerer, K. D. Angielczyk, & J. Fröbisch (Eds.), *Early Evolutionary History of the Synapsida* (pp. 93–138). Dordrecht: Springer.
- Barghusen, H. R. (1986). On the evolutionary origin of the therian *tensor veli palatini* and *tensor tympani* muscles. In N. Hotton, P. D. Maclean, J. J. Roth, & E. C. Roth (Eds.), *The ecology and biology of mammal-like reptiles* (pp. 253–262). Washington, D.C.: Smithsonian Institution Press.
- Barker, C. T., Naish, D., Newham, E., Katsamenis, O. L., & Dyke, G. (2017). Complex neuroanatomy in the rostrum of the Isle of Wight theropod *Neovenator salerii*. *Scientific Reports*, 7, 3749.
- Barry, T. H. (1974). A new dicynodont ancestor from the Upper Eccles. *Annals of the South African Museum*, 64, 117–136.
- Benoit, J., Abdala, F., Van den Brandt, M. J., Manger, P. R., & Rubidge, B. S. (2015). Physiological implications of the abnormal absence of the parietal foramen in a Late Permian cynodont (Therapsida). *The Science of Nature (Naturwissenschaften)*, 102(11–12), 69.
- Benoit, J., Fernandez, V., Manger, P. R., & Rubidge, B. S. (2016b). Cranial bosses of *Choerosaurus dejageri* (Therapsida, Therocephalia): Earliest evidence of cranial display structures in eutheriodonts. *PLoS One*, 11(8), e0161457.
- Benoit, J., Manger, P. R., & Rubidge, B. S. (2016a). Palaeoneurological clues to the evolution of defining mammalian soft tissue traits. *Scientific Reports*, 6, 25604.
- Benoit, J., Manger, P. R., Norton, L. A., Fernandez, V., & Rubidge, B. S. (2017a). Synchrotron scanning reveals the palaeoneurology of the head-butting *Moschops capensis* (Therapsida, Dinocephalia). *PeerJ*, 5, e3496.
- Benoit, J., Norton, L. A., Manger, P. R., & Rubidge, B. S. (2017b). Reappraisal of the envenoming capacity of *Euchambersia mirabilis* (Therapsida, Therocephalia) using µCT-scanning techniques. *PLoS One*, 12(2), e0172047.
- Bellairs, A. D. A. (1949). Observations on the snout of *Varanus*, and a comparison with that of other lizards and snakes. *Journal of Anatomy*, 83, 116–146.
- Billet, G., Hautier, L., Asher, R., Schwarz, C., Crumpton, N., Martin, T., & Ruf, I. (2012). High morphological variation of vestibular system accompanies slow and infrequent locomotion in three-toed sloths. *Proceedings of the Royal Society B: Biological Sciences*, 279, 3932–3939.
- Boos, A. D. S., Kammerer, C. F., Schultz, C. L., Soares, M. B., & Ilha, A. L. R. (2016). A new dicynodont (Therapsida: Anomodontia) from the Permian of southern Brazil and its implications for bidental origins. *PLoS One*, 11(5), e0155000.
- Botha, J. (2003). Biological aspects of the Permian dicynodont *Oudenodon* (Therapsida: Dicynodontia) deduced from bone histology and cross-sectional geometry. *Palaeontologia Africana*, 39, 37–44.
- Botha-Brink, J. (2017). Burrowing in *Lystrosaurus*: Preadaptation to a postextinction environment?. *Journal of Vertebrate Paleontology*, 37(5), e1365080.
- Botha, J., & Angielczyk, K. D. (2007). An integrative approach to distinguishing the Late Permian dicynodont species *Oudenodon bainii* and *Tropidostoma microtrema* (Therapsida: Anomodontia). *Palaeontology*, 50(5), 1175–1209.
- Botha-Brink, J., & Angielczyk, K. D. (2010). Do extraordinarily high growth rates in Permo-Triassic dicynodonts (Therapsida, Anomodontia) explain their success before and after the end-Permian extinction? *Zoological Journal of the Linnean Society*, 160, 341–365.
- Botha, J., & Smith R. M. H. (2007). *Lystrosaurus* species composition across the Permo-Triassic boundary of South Africa. *Lethaia*, 40, 125–137.
- Brinkman, D. B. (1981). The structure and relationships of the dromaeosaurs (Reptilia: Therapsida). *Breviora*, 465, 1–34.
- Brochu, C. A. (2003). Osteology of *Tyrannosaurus rex*: Insights from a nearly complete skeleton and high-resolution computed tomographic analysis of the skull. *Journal of Vertebrate Paleontology*, 7(sup4), 1–138.
- Broom, R. (1903a). On the classification of the theriodonts and their allies. *Report of the South African Association for the Advancement of Science*, 1, 286–295.
- Broom, R. (1903b). On the structure of the shoulder girdle in *Lystrosaurus*. *Annals of the South African Museum*, 4, 139–141.
- Broom, R. (1932). *The mammal-like reptiles of South Africa and the origin of mammals*. London: H. F. and G. Witherby.
- Brink, A. S. (1951). On the genus *Lystrosaurus* Cope. *Transactions of the Royal Society of South Africa*, 33(1), 107–120.
- Buchtová, M., Páč, L., Knotek, Z., & Tichy, F. (2009). Complex sensory corpuscles in the upper jaw of Horsfield's Tortoise (*Testudo horsfieldii*). *Acta Veterinaria Brno*, 78, 193–197.
- Camp, G. L. (1956). Triassic dicynodont reptiles. Part II. Triassic dicynodonts compared. *Memoirs of the University of California*, 13, 305–348.
- Canoville, A., & Laurin, M. (2010). Evolution of humeral microanatomy and lifestyle in amniotes, and some comments on paleobiological inferences. *Biological Journal of the Linnean Society*, 100, 384–406.
- Castanhinha, R., Araújo, R., Júnior, L. C., Angielczyk, K. D., Martins, G. G., Martins, R. M. S., ... Wilde, F. (2013). Bringing dicynodonts back to life: Paleobiology and anatomy of a new emydopoid genus from the Upper Permian of Mozambique. *PLoS One*, 8(12), e80974.
- Cisneros, J. C., Abdala, F., Rubidge, B. S., Dentzen-Dias, P. C., & Bueno Ade, O. (2011). Dental occlusion in a 260-million-year-old therapsid with saber canines from the Permian of Brazil. *Science*, 331(6024), 1603–1605.
- Cisneros, J. C., Abdala, F., Jashashvili, T., Bueno, A. O., & Dentzen-Dias, P. (2015). *Tiarajudens eccentricus* and *Anomocephalus africanus*, two bizarre anomodonts (Synapsida, Therapsida) with dental occlusion from the Permian of Gondwana. *Royal Society Open Science*, 2, 150090.
- Cluver, M. A. (1970). The palate and mandible in some specimens of *Dicynodon testudirostris* Broom and Haughton (Reptilia, Therapsida). *Annals of the South African Museum*, 56, 133–153.
- Cluver, M. A. (1971). The cranial morphology of the dicynodont genus *Lystrosaurus*. *Annals of the South African Museum*, 56, 155–274.
- Cluver, M. A. (1974). The cranial morphology of the Lower Triassic dicynodont *Myosaurus gracilis*. *Annals of the South African Museum*, 66, 35–54.
- Cluver, M. A. (1978). The skeleton of the mammal-like reptile *Cistecephalus* with evidence for a fossorial mode of life. *Annals of the South African Museum*, 76, 213–246.
- Cox, C. B. (1972). A new digging dicynodont from the Upper Permian of Tanzania. In K. A. Josey & T. S. Kemp (Eds.), *Studies in vertebrate evolution* (pp. 173–189). Edinburgh: Oliver and Boyd.
- Cox, C. B., & Angielczyk, K. D. (2015). A new endothiodont dicynodont (Therapsida, Anomodontia) from the Permian Ruhuhu Formation (Songea Group) of Tanzania and its feeding system. *Journal of Vertebrate Paleontology*, 35(4), e935388.
- Cox, B. (1998). The jaw function and adaptive radiation of the dicynodont mammal-like reptiles of the Karoo basin of South Africa. *Zoological Journal of the Linnean Society*, 122(1–2), 349–384.
- Crompton, A. W., & Hotton, N. (1967). Functional morphology of the masticatory apparatus of two dicynodonts (Reptilia, Therapsida). *Postilla*, 109, 1–51.

- Crompton, A. W., Musinsky, C., & Owerkowicz, T. (2015). The Evolution of the Mammalian Nose. In K. Dial, N. H. Shubin, & E. L. Brainerd (Eds.), *Great transformations in vertebrate evolution* (pp. 189–205). Chicago: University of Chicago Press.
- Crompton, A. W., Owerkowicz, T., Bhullar, B.-A., & Musinsky, C. (2017). Structure of the nasal region of non-mammalian cynodonts and mammaliforms: Speculations on the evolution of mammalian endothermy. *Journal of Vertebrate Paleontology*, 37, e1269116.
- Dubbeldam, J. L. (1998). The sensory trigeminal system in birds: Input, organization and effects of peripheral damage. A review. *The Journal of Metabolic Diseases*, 106(5), 338–345.
- During von, M., & Miller, M. R. (1979). Sensory nerve endings of the skin and deeper structures. In C. Gans, R. G. Northcutt, & P. Ulinski (Eds.), *Biology of the reptilia Volume 9, Neurology* (pp. 407–411). New York: Academic Press.
- Estes, R. (1961). Cranial anatomy of the cynodont reptile *Thrinaxodon liorhinus*. *Bulletin of the Museum of Comparative Zoology*, 125, 165–180.
- Fernandez, V., Abdala, F., Carlson, K. J., Cook, D. C., Rubidge, B. S., Yates, A., & Tafforeau, P. (2013). Synchrotron reveals early triassic odd couple: Injured amphibian and aestivating therapsid share burrow. *PLoS One*, 8(6), e64978.
- Fröbisch, J. (2006). Locomotion in derived dicynodonts (Synapsida, Anomodontia): A functional analysis of the pelvic girdle and hind limb of *Tetraponeras njalilus*. *Canadian Journal of Earth Sciences*, 43(9), 1297–1308.
- Fröbisch, J. (2009). Composition and similarity of global anomodont-bearing tetrapod faunas. *Earth-Science Reviews*, 95(3–4), 119–157.
- Fröbisch, J. (2008). Global taxonomic diversity of anomodonts (Tetrapoda, Therapsida) and the terrestrial rock record across the Permian-Triassic boundary. *PLoS One*, 3(11), e3733.
- Fröbisch, J. (2013). Vertebrate diversity across the end-Permian extinction—separating biological and geological signals. *Palaeogeography, Palaeoclimatology, Palaeoecology*, 372, 50–61.
- Fröbisch, J., & Reisz, R. R. (2009). The Late Permian herbivore Suminia and the early evolution of arboreality in terrestrial vertebrate ecosystems. *Proceedings of the Royal Society B: Biological Sciences*, 276 (1673), 3611–3618.
- Fröbisch, J., & Reisz, R. R. (2011). The postcranial anatomy of *Suminia getmanovi* (Synapsida: Anomodontia), the earliest known arboreal tetrapod. *Zoological Journal of the Linnean Society*, 162, 661–698.
- Germain, D., & Laurin, M. (2005). Microanatomy of the radius and life-style in amniotes (Vertebrata, Tetrapoda). *Zoologica Scripta*, 34, 335–350.
- Grine, F. E., Forster, C. A., Cluver, M. A., & Georgi, J. A. (2006). Cranial variability, ontogeny, and taxonomy of *Lystrosaurus* from the Karoo Basin of South Africa. In M. T. Carrano, T. J. Gaudin, R. W. Blob & J. R. Wible (Eds.), *Amniote paleobiology: Perspectives on the evolution of mammals, birds, and reptiles*. (pp. 432–503). Chicago: University of Chicago Press.
- Groenewald, G. H. (1991). Burrow casts from the *Lystrosaurus-Procolophon* Assemblage Zone, Karoo Sequence, South Africa. *Koedoe*, 34(1), 13–22.
- Hammer, W. R., & Cosgriff, J. W. (1981). *Myosaurus gracilis*, an Anomodont Reptile from the Lower Triassic of Antarctica and South Africa. *Journal of Paleontology*, 55, 410–424.
- Higashiyama, H., & Kuratani, S. (2014). On the maxillary nerve. *Journal of Morphology*, 275, 17–38.
- Hieronymus, T. L., Witmer, L. M., Tanke, D. H., & Currie, P. J. (2009). The facial integument of centrosaurine ceratopsids: Morphological and histological correlates of novel skin structures. *The Anatomical Record*, 292, 1370–1396.
- Hotton, N. III. (1986). Dicynodonts and their role as primary consumers. In N. Hotton, III., P. D. MacLean, J. J. Roth, & E. C. Roth (Eds.), *The ecology and biology of mammal-like reptiles* (pp. 71–82). Washington, D.C: Smithsonian Institution Press.
- Huxley, T. H. (1859). On a new species of *Dicynodon* (*D. Murrayi*), from near Colesberg, South Africa; and on the structure of the skull in dicynodonts. *The Quarterly Journal of the Geological Society of London*, 15(1–2), 555–658.
- Irmis, R. B., & Whiteside, J. H. (2012). Delayed recovery of non-marine tetrapods after the end-Permian mass extinction tracks global carbon cycle. *Proceedings of the Royal Society B: Biological Sciences*, 279, 1310–1318.
- Ivakhnenko, M. F. (1996). Primitive anomodonts, venyukoviids, from the Late Permian of Eastern Europe. *Paleontological Journal*, 30, 77–84.
- Ivakhnenko, M. F. (2001). Tetrapods from the East European Placket—Late Paleozoic Natural Territorial Complex. *Trudy Paleontologičeskogo Instituta Rossijskoi Akademii Nauk [Transactions of the Paleontological Institute of the Russian Academy of Sciences]*, 283, 1–200.
- Jasinoski, S. C., & Chinsamy-Turan, A. (2012). Biological inferences of the cranial microstructure of the dicynodonts *Oudenodon* and *Lystrosaurus*. In A. Chinsamy-Turan (Ed.), *Forerunners of mammals: Radiation, histology, biology* (pp. 149–178). Bloomington: Indiana University Press.
- Jasinoski, S. C., Rayfield, E. J., & Chinsamy, A. (2009). Comparative feeding biomechanics of *Lystrosaurus* and the generalized dicynodont *Oudenodon*. *The Anatomical Record*, 292, 862–874.
- Jasinoski, S. C., Rayfield, E. J., & Chinsamy, A. (2010a). Functional implications of dicynodont cranial suture morphology. *Journal of Morphology*, 271, 705–728.
- Jasinoski, S. C., Rayfield, E. J., & Chinsamy, A. (2010b). Mechanics of the Scarf Premaxilla-Nasal Suture in the Snout of *Lystrosaurus*. *Journal of Vertebrate Paleontology*, 30, 1283–1288.
- Kammerer, C. F., & Angielczyk, K. D. (2009). A proposed higher taxonomy of anomodont therapsids. *Zootaxa*, 2018, 1–24.
- Kammerer, C. F., Angielczyk, K. D., & Fröbisch, J. (2011). A comprehensive taxonomic revision of *Dicynodon* (Therapsida, Anomodontia) and its implications for dicynodont phylogeny, biogeography, and biostratigraphy. *Journal of Vertebrate Paleontology*, 31, 1–158.
- Kammerer, C. F., Fröbisch, J., & Angielczyk, K. D. (2013). On the validity and phylogenetic position of *Eubrachiosaurus browni*, a Kannemeyeriform Dicynodont (Anomodontia) from Triassic North America. *PLoS One*, 8(5), e64203.
- Kemp, T. S. (1982). *Mammal-like reptiles and the origin of mammals*. London: Academic Press.
- Keyser, A. W. (1965). The morphology of the anomodont genus *Cistecephalus* Owen, 1876. University of Pretoria, Master's dissertation.
- Keyser, A. W. (1973). A preliminary study of the type area of the *Cistecephalus* Zone of the Beaufort Series, and a revision of the anomodont family Cistecephalidae. *Geological Survey of South Africa Memoir*, 62, 1–71.
- Keyser, A. W. (1993). A re-evaluation of the smaller Endothiodontidae. *Memoirs of the Geological Survey of South Africa*, 82, 1–53.
- King, G. M. (1985). The postcranial skeleton of *Kingoria nowacki* (von Huene) (Therapsida: Dicynodontia). *Zoological Journal of the Linnean Society*, 84(3), 263–289.
- King, G. (1988). Anomodontia. In P. Wellnhofer (Ed.), *Encyclopedia of paleoherpetology*. (pp. 1–174). Stuttgart: Gustav Fischer.

- King, G. M. (1990). *The dicynodonts: A study in paleobiology*. London: Chapman and Hall.
- King, G. M. (1994). The early anomodont *Venjukovia* and the evolution of the anomodont skull. *Journal of Zoology*, 232(4), 651–673.
- King, G. M., Oelofsen, B. W., & Rubidge, B. S. (1989). The evolution of the dicynodont feeding system. *Zoological Journal of the Linnean Society*, 96, 185–212.
- King, G. M. (1991). The aquatic *Lystrosaurus*: a palaeontological myth. *Historical Biology*, 4, 285–321.
- King, G. M., & Cluver, M. A. (1991). The aquatic *Lystrosaurus*: An alternative lifestyle. *Historical Biology*, 4, 323–341.
- Krapovickas, V., Mancuso, A. C., Marsicano, C. A., Domnanovich, N. S., & Schultz, C. L. (2013). Large tetrapod burrows from the Middle Triassic of Argentina: A behavioural adaptation to seasonal semi-arid climate? *Lethaia*, 46, 154–169.
- Kurkin, A. A. (2000). New dicynodonts from the Upper Permian of the Vyatka Basin. *Paleontological Journal*, 34, S203–S210.
- Laaß, M. (2015). Bone-conduction hearing and seismic sensitivity of the late Permian anomodont *Kawingasaurus fossilis*. *Journal of Morphology*, 276(2), 121–143.
- Laaß, M., & Schillinger, B. (2015). Reconstructing the auditory apparatus of therapsids by means of neutron tomography. *Physics Procedia*, 69, 628–635.
- Laaß, M., & Kaestner, A. (2017). Evidence for convergent evolution of a structure comparable to the mammalian neocortex in a Late Permian therapsid. *Journal of Morphology*, 278, 1033–1057.
- Lee, M. S. Y. (1997). The evolution of beaks in reptiles: A proposed evolutionary constraint. *Evolutionary Theory*, 11, 249–254.
- Leitch, D. B., & Catania, K. C. (2012). Structure, innervation and response properties of integumentary sensory organs in crocodilians. *Journal of Experimental Biology*, 215, 4217–4230.
- Liu, J., Rubidge, B., & Li, J. (2010). A new specimen of *Biseridens qilianicus* indicates its phylogenetic position as the most basal anomodont. *Proceedings of the Royal Society B: Biological Sciences*, 277, 285–292.
- Lungmus, J. K., Angielczyk, K. D., Sidor, C. A., Nesbitt, S. J., Smith, R. M., Steyer, J.-S., ... Tolan, S. (2015). A new cistecephalid dicynodont (Therapsida, Anaomodontia) from the Mid-Zambezi Basin (Zambia) and its fossorial adaptations. *Society of Vertebrate Paleontology 75th Annual Meeting, Dallas, Texas*.
- Manger, P. R., & Pettigrew, J. D. (1996). Ultrastructure, number, distribution and innervation of electroreceptors and mechanoreceptors in the bill skin of the platypus. *Brain Behavior and Evolution*, 48, 27–54.
- Manger, P. R., & Pettigrew, J. D. (1995). Electroreception and the feeding behaviour of the platypus (*Ornithorhynchus anatinus*: Monotremata: Mammalia). *Philosophical Transactions of the Royal Society B: Biological Sciences*, 347, 359–381.
- Modesto, S. P., & Botha-Brink, J. (2010). A burrow cast with *Lystrosaurus* skeletal remains from the Lower Triassic of South Africa. *Journal of Vertebrate Paleontology*, 25, 274–281.
- Modesto, S. P., Rubidge, B. S., Visser, I., & Welman, J. (2003). A new basal dicynodont from the Upper Permian of South Africa. *Palaeontology*, 46, 211–223.
- Nasterlack, T., Canoville, A., & Chinsamy, A. (2012). New insights into the biology of the Permian genus *Cistecephalus* (Therapsida, Dicynodontia). *Journal of Vertebrate Paleontology*, 32, 1396–1410.
- Nieuwenhuys, R., Ten Donkelaar, H. J., & Nicholson, C. (1998). *The central nervous system of vertebrates*. Berlin: Springer.
- Maddison, W. P., & Maddison, D. R. (2017). Mesquite: A modular system for evolutionary analysis. Version 3.2 <http://mesquiteproject.org>
- Modesto, S., & Rubidge, B. (2000). A basal anomodont therapsid from the lower Beaufort Group, Upper Permian of South Africa. *Journal of Vertebrate Paleontology*, 20, 515–521.
- Olroyd, S. L., Sidor, C. A., & Angielczyk, K. D. (In Press) New materials of the enigmatic dicynodont *Abajudon kaayai* (Therapsida, Anomodontia) from the lower Madumabisa Mudstone Formation, middle Permian of Zambia. *Journal of Vertebrate Paleontology*.
- Owen, R. (1845). Report on the Reptilian Fossils of South Africa: PART I.—Description of certain Fossil Crania, discovered by A. G. Bain, Esq., in Sandstone Rocks at the South-eastern extremity of Africa, referable to different species of an Extinct genus of Reptilia (Dicynodon), and indicative of a new Tribe or Sub-order of Sauria. *Transactions of the Geological Society of London*, s2, 59–84.
- Owen, R. (1860). On the orders of fossil and recent Reptilia, and their distribution in time. *Report of the British Association for the Advancement of Science*, 1859, 153–166.
- Owen, R. (1866). *The anatomy of vertebrates, Vol. 1: Fishes and reptiles*. London: Longmans, Green, and Co.
- Ray, S., Chinsamy, A., & Bandyopadhyay, S. (2005). *Lystrosaurus murrayi* (Therapsida, Dicynodontia): Bone histology, growth, and lifestyle adaptations. *Palaeontology*, 48, 1169–1185.
- Rayner, R. J. (1992). *Phyllotheca*: The pastures of the Late Permian. *Palaeogeography, Palaeoclimatology, Palaeoecology*, 92(1–2), 31–40.
- Rodella, L. F., Buffoli, B., Labanca, M., & Rezzani, R. (2012). A review of the mandibular and maxillary nerve supplies and their clinical relevance. *Archives Oral Biology*, 57, 323–334.
- Rubidge, B. S. (1984). The cranial morphology and palaeoenvironment of *Eodicynodon* Barry (Therapsida: Dicynodontia). *Navorsinge Van Die Nasionale Museum Bloemfontein, South Africa*, 4(14), 325–402.
- Rubidge, B. S. (1990a). A new vertebrate biozone at the base of the Beaufort Group. *Palaeontologia Africana*, 27, 17–20.
- Rubidge, B. S. (1990b). Redescription of the cranial morphology of *Eodicynodon oosthuizeni* (Therapsida: Dicynodontia). *Navorsinge Van Die Nasionale Museum Bloemfontein, South Africa*, 7, 1–25.
- Rubidge, B. S., & Hopson, J. A. (1996). A primitive anomodont therapsid from the base of the Beaufort Group (Upper Permian) of South Africa. *Zoological Journal of the Linnean Society*, 117, 115–139.
- Ruta, M., Angielczyk, K. D., Fröbisch, J., & Benton, M. J. (2013). Decoupling of morphological disparity and taxic diversity during the adaptive radiation of anomodont therapsids. *Proceedings of the Royal Society B: Biological Sciences*, 280(1768), 20131071.
- Rybaczynski, N. (2000). Cranial anatomy and phylogenetic position of *Suminia getmanovi*, a basal anomodont (Amniota: Therapsida) from the Late Permian of Eastern Europe. *Zoological Journal of the Linnean Society*, 130(3), 329–373.
- Sidor, C. A., & Smith, R. M. H. (2007). A second burnetiamorph therapsid from the Permian Teekloof Formation of South Africa and its associated fauna. *Journal of Vertebrate Paleontology*, 27, 420–430.
- Smith, R. M. H., Rubidge, B. S., & van der Walt, M. (2012). Therapsid biodiversity patterns and environments of the Karoo Basin, South Africa. In A. Chinsamy (Ed.), *Forerunners of mammals: Radiation, histology, biology*. (pp. 223–246). Bloomington and Indianapolis: Indiana University Press.
- Sullivan, C., Reisz, R. R., & Smith, R. M. H. (2003). The Permian mammal-like herbivore *Dictyodon*, the oldest known example of sexually dimorphic armament. *Proceedings of the Royal Society B: Biological Sciences*, 270, 173–178.

- Sullivan, C., & Reisz, R. R. (2005). Cranial anatomy and taxonomy of the Late Permian dicynodont *Diictodon*. *Annals of Carnegie Museum*, 74, 45–75.
- Surkov, M. V. (2006). The first evidence of tactile sensor zones among dicynodonts. *Proceedings of Saratov University, New Series, Earth Sciences*, 6, 91–95.
- Tatarinov, L. P. (1976). *Morphological evolution of the Theriodonts and the general problems of Phylogenetics*. Moscow: NAUKA.
- Tatarinov, L. P. (1999). The nasal cavity, maxillary sensory system, and certain brain features of the ictidosuchoidea (reptilia, theriodontia). *Paleontological Journal*, 33, 99–110.
- Thulborn, T., & Turner, S. (2003). The last dicynodont: An Australina Cretaceous relict. *Proceedings of the Royal Society B: Biological Sciences*, 270(1518), 985–993.
- Watson, D. M. S. (1912). The skeleton of *Lystrosaurus*. *Records of the Albany Museum*, 2, 287–299.
- Watson, D. M. S. (1913). The limbs of *Lystrosaurus*. *Geological Magazine*, 10(06), 256–258.
- Watson, D. M. S. (1948). *Dicynodon* and its allies. *Proceedings of the Zoological Society of London*, 118, 823–877.
- Watson, D. M. S., & Romer, A. S. (1956). A classification of therapsid reptiles. *Bulletin of the Museum of Comparative Zoology*, 114, 35–89.
- Witmer, L. M. (1995). Homology of facial structures in extant archosaurs (birds and crocodilians), with special reference to paranasal pneumaticity and nasal conchae. *Journal of Morphology*, 225(3), 269–327.

SUPPORTING INFORMATION

Additional Supporting Information may be found online in the supporting information tab for this article.

How to cite this article: Benoit J, Angielczyk KD, Miyamae JA, Manger P, Fernandez V, Rubidge B. Evolution of facial innervation in anomodont therapsids (Synapsida): Insights from X-ray computerized microtomography. *Journal of Morphology*. 2018;279:673–701. <https://doi.org/10.1002/jmor.20804>